NATIONAL ADVISORY COMMITTEE FOR AERONAUTICS

TECHNICAL NOTE 3462

TENSILE PROPERTIES OF 7075-T6 AND 2024-T3 ALUMINUM-ALLOY SHEET HEATED AT UNIFORM TEMPERATURE RATES UNDER CONSTANT LOAD

By George J. Heimerl and John E. Inge

Langley Aeronautical Laboratory
Langley Field, Va.

Washington
July 1955

1G

NATIONAL ADVISORY COMMITTEE FOR AERONAUTICS

TECHNICAL NOTE 3462

TENSILE PROPERTIES OF 7075-T6 AND 2024-T3 ALUMINUM-ALLOY SHEET HEATED AT UNIFORM TEMPERATURE RATES UNDER CONSTANT LOAD

By George J. Heimerl and John E. Inge

SUMMARY

Results are presented of tests to determine the effect of heating at uniform temperature rates from 0.2° F to 100° F per second on the tensile properties of 7075-T6 (formerly 75S-T6) and 2024-T3 (formerly 24S-T3) aluminum-alloy sheet under constant-load conditions. The temperatures at which yield and rupture occurred were determined for various stress levels. Yield and rupture stresses, obtained under rapid-heating and constant-load conditions, are compared with the results of elevated-temperature tensile stress-strain tests of the same materials for 1/2-hour exposure. Linear and reciprocal temperature-rate parameters are derived from the data. Master yield- and rupture-stress curves, based upon the linear temperature parameter, are presented with which yield and rupture stresses or temperatures may be predicted for these materials for temperature rates from 0.2° F to 100° F per second. A description of the test equipment is included.

INTRODUCTION

Aircraft and missile structural materials may be subjected to rapid heating while under load because of aerodynamic heating at supersonic speeds. Temperatures and temperature rates of the materials may vary widely.

In order to provide information on the tensile properties of materials under rapid-heating conditions, some tests have been made of a number of steels, titanium and aluminum alloys, and heat-resistant materials which were heated at high temperature rates under constant-load conditions (refs. 1 to 6). The results obtained so far indicate that, in general, metals and alloys can withstand substantially higher stresses at a given temperature when heated at 100° F to 200° F per second under constant-load conditions than when loaded after the material has been exposed 1/2 hour or longer at constant temperature. Increasing the temperature rate from 200° F to 2,000° F per second or more results in only a small additional increase in strength.

Although temperature rates below 100° F per second are presently being encountered, information on the properties of materials when heated at these lower rates is lacking. Consequently, an investigation was undertaken at the Langley Aeronautical Laboratory to determine the tensile properties of some aircraft structural materials when heated at temperature rates up to 100° F per second. The results of tests of 7075-T6 and 2024-T3 aluminum-alloy sheet, heated at rates from 0.2° F to 100° F per second under constant-tensile-load conditions, are presented herein. In these tests the load is applied first, and then the specimen is heated electrically at a predetermined constant temperature rate until failure occurs. Strain-temperature histories are obtained which provide the basis for the determination of yield and rupture temperatures. The results of the rapid-heating tests are compared with conventional elevated-temperature tensile stress-strain data obtained for the same materials after 1/2-hour exposure. Parameters are derived which take into account the effects of temperature rate on the stress and temperature at which yield and rupture occur.

TEST PROCEDURE

Specimens

Stress-strain and rapid-heating tensile test specimens were cut from 0.125-inch 7075-T6 and 2024-T3 aluminum-alloy sheet with the longitudinal axis of the specimen parallel to the rolling direction. The specimens for each material were taken from a single sheet.

The dimensions of the stress-strain and rapid-heating specimens are shown in figure 1. The relatively long reduced section of the rapid-heating specimen was arrived at after considerable experimentation with shorter specimens with which excessive temperature gradients were obtained over the 1-inch gage length of the reduced section. Attempts to improve the gradient condition for the short specimens by the use of auxiliary end-heater systems were not generally successful. Although the shape shown for the rapid-heating specimen was fairly satisfactory for use with the extensometer system employed and the aluminum-alloy materials, later experience indicated that the long, parallel reduced section may not be the best design for other materials having appreciably different thermal properties. In such instances it was found necessary to reduce the temperatures outside the center region by means of cooling plates clamped to the faces of the specimen in order that fracture would occur in or near the gage-length region.

Methods of Testing

Short-time stress-strain tests.- Conventional short-time elevated-temperature tensile stress-strain tests were made for the 7075-T6 and 2024-T3 aluminum-alloy-sheet materials. The specimens were exposed 1/2 hour to the test temperature before the load was applied at a strain rate of approximately 0.002 per minute. The equipment used for these tests is shown and described in reference 7.

Rapid-heating tests.- In the rapid-heating tests, the specimens were loaded and then heated by passing a low-voltage high-amperage alternating current directly through the specimen. The specimen strain was measured over a 1-inch gage length by an extensometer system. The loading, heating, and strain-measuring equipment is described in the appendix and illustrated in figures 2 to 5. Information on the specimen temperature gradient is also given in the appendix and shown in figure 6.

Specimens were first loaded to selected stress levels and then heated at nominal constant temperature rates of 1/4°, 2°, 15°, 60°, and 100° F per second until failure occurred. Temperature-time records were obtained to failure, and strain-time records to failure were obtained except where the limits of the recorder chart were exceeded. Strains were recorded on initial loading and provided a check on the accuracy and reliability of the measurement, inasmuch as these strains could be calculated beforehand. The sensitivity for the strain measurement (either 0.002 or 0.005 per inch of chart) was selected to provide the most desirable slope on the strain-time record which could be obtained for the particular combination of stress level, temperature rate, and chart speed used for the test. The extensometer error was found to be within less than ±2 percent.

The desired temperature rate was laid out on a recorder chart prior to making the test. This straight line was then followed as closely as possible by manual adjustment of the voltage regulator. (See the appendix.) The approximate setting required for a particular temperature rate was determined by a few trial runs at low temperatures prior to the test. Manual control of the regulator was required for rates up to 60° F per second because of the tendency for the rate to drop off as the temperature increased for a constant regulator setting. At higher rates, no adjustments were needed once the proper initial setting had been determined.

In order to illustrate the nature of the test results and how they are processed, strain- and temperature-time curves are shown in figure 7 for two tests of 7075-T6 aluminum alloy at 40 ksi for temperature rates of 0.23° F and 54° F per second. The heating rate is determined from the slope of the temperature-time curve. For cases in which the rate was not quite linear, an average rate was used, which approximated the temperature-time curve about up to the temperature at which plastic flow

began. Strain-temperature curves were constructed from the strain- and temperature-time records by determining simultaneous values of strain and temperature at appropriate time intervals throughout the test. Strain-temperature curves for the tests in figure 7 are given in figure 8. The strain-temperature curves coincide up to about 250° F, and the initial strains obtained upon loading before heating agree with the calculated values. In some cases the strain-temperature curves, although parallel, did not coincide exactly and some variation was obtained in the initial strains for the same stress level. In such cases, the strains were adjusted by adding or subtracting a small constant amount in order to eliminate the initial scatter. The adjustment in strain was at the most only ±0.0002.

The method of determining the yield temperature is also shown in figure 8. The initial strain-temperature histories are identical up to about 250° F for both of the temperature rates and follow the curve for thermal expansion and change in elastic modulus for the material. Divergence upward from this curve indicates the plastic flow which occurs at the higher temperatures. Yield temperatures are determined by the intersection of a 0.2-percent-offset line with the test curves, which is drawn parallel to and 0.2 percent above the curve for thermal expansion and change in elastic modulus. The latter curve was calculated and found to be in close agreement with the test results at temperatures below those at which plastic flow began. The curve for thermal expansion and change in modulus can also be extrapolated from the test results at the lower temperatures by using the similar curve at the next lower stress level as a guide inasmuch as these curves are nearly parallel when the stress differences are small. The latter method was used above about 600° F because of the uncertainty as to moduli values at high temperatures and the fact that different thermal-expansion curves were obtained for the different temperature rates at the higher temperatures.

The rupture temperature was taken as the maximum temperature obtained at the midposition at the instant of rupture. When rupture occurred, the circuit was broken so that heating stopped immediately. (See fig. 7.) Because the temperature just outside the gage length was somewhat higher than that inside the region (see the appendix), failure usually occurred outside the gage length. Rupture temperatures, measured at the midposition, are therefore somewhat conservative.

TEST RESULTS AND DISCUSSION

The results of the elevated-temperature tensile stress-strain tests of 7075-T6 and 2024-T3 aluminum-alloy sheet are given in table 1. Tensile stress-strain curves for these materials are shown in figure 9 for temperatures up to 685° F. (The 0.2-percent-offset yield stresses are indicated by the tick marks.) These data are for 1/2-hour exposure at constant temperature and were obtained at a constant strain rate of 0.002 per minute.

The results of the rapid-heating tests are given in tables 2 and 3 and figures 10 to 19. Table 2 and figures 10, 12, 14, 16, and 18 apply to 7075-T6 aluminum alloy, and table 3 and figures 11, 13, 15, 17, and 19 apply to 2024-T3 aluminum alloy. Average values of the thermal coefficient of expansion for these materials obtained under rapid-heating conditions are given in table 4.

Strain-Temperature Histories

Strain-temperature histories for 7075-T6 and 2024-T3 aluminum alloy are shown in figures 10 and 11, respectively, for nominal temperature rates of 1/4°, 2°, 15°, 60°, and 100° F per second at various stress levels. Yield temperatures (0.2-percent offset) are indicated by the tick marks, and actual temperature rates are given for each test. At each stress level, families of curves are obtained in which the yield temperatures generally increase with increases in temperature rate, and all the test curves merge into a single curve at the lower temperatures regardless of the temperature rate. The single curves coincide at each stress level at the lower temperatures with the calculated curves for thermal expansion and change in modulus, which are shown by the light curves extending to the right in each case. The upward deviation of the test curves from the curve for thermal expansion and change in modulus is a measure of the plastic flow. The strains are the total strains which include the initial elastic and plastic strains, the thermal strains, the elastic strains resulting from a decrease in modulus with temperature, and the plastic strains that occur as the temperature increases.

The results for 7075-T6 (fig. 10) are very uniform and regular in pattern. Yield temperatures increase with increases in the temperature rate at each stress level. The results for 2024-T3 (fig. 11) are not so regular or consistent as those for 7075-T6 at the different stress levels. At 50 ksi, for example, the test results for 2024-T3 follow approximately a single curve all the way up to about the yield temperature, after which they fall into a more or less normal or typical pattern in which the temperatures for a given strain increase with increasing temperature rate. Other irregularities are also apparent in the test results for 2024-T3. For example, at 40 ksi and a temperature rate of 0.23° F per second, the strain-temperature curve deviates irregularly to the right and crosses the other curves at strains above about 2 percent. At 16.5 ksi, the curves for temperature rates of 15° F and 53° F per second also cross each other in an irregular manner. Additional tests were made to check these peculiarities but these gave essentially the same results. This behavior of 2024-T3 is presumably due to its age-hardening characteristics which, under these variable temperature conditions, can be expected to increase or alter the strength of the material.

The tests at 0.4 ksi are essentially thermal-expansion tests (figs. 10 and 11). At temperatures above about 400° F for 7075-T6 and 300° F for

2024-T3, the thermal-expansion curves obtained at 58° F to 60° F per second are appreciably above those obtained at 0.23° F per second for both materials. Such differences in thermal-expansion curves at different temperature rates could possibly occur because the materials are unstable or because of inaccuracies of testing. In order to eliminate the latter possibility, additional thermal-expansion tests were made on a stabilized specimen of 7075-T6. This specimen was repeatedly heated slowly to 750° F and cooled until the same thermal-expansion curve was obtained at a temperature rate of 2° F per second both on heating and cooling. The temperature rate was then increased to 60° F per second, and the same thermal-expansion curve was obtained (fig. 10). The possibility of variations due to test inaccuracies at different temperature rates was therefore eliminated. The thermal-expansion curve for the stabilized materials falls between the results for the two temperature rates for the unstable material. Values of the average coefficient of expansion for 7075-T6 and 2024-T3, calculated from the results for 0.4 ksi (figs. 10 and 11), are given in table 4.

Yield Temperatures and Stresses

The variation of yield temperature with the temperature rate, plotted on a logarithmic scale, is shown in figures 12 and 13 for 7075-T6 and 2024-T3, respectively, for the different stress levels. For 7075-T6 (fig. 12), very little scatter is evident and the curves are nearly linear. Yield temperatures for a given stress level are therefore proportional to the logarithm of the temperature rate. For 2024-T3 (fig. 13), considerably more scatter is found and the curves are not so linear. Yield temperatures are only approximately proportional to the logarithm of the temperature rate in this case.

Yield stresses, defined as those stresses at which yield temperatures occur under rapid-heating conditions, are shown in figure 14 for 7075-T6 for temperature rates of 0.2°, 2°, 20°, 60°, and 100° F per second. This figure was constructed for these arbitrary rates by determining the yield temperatures from the experimental curves of figure 12 for the different stress levels. The variation of the yield stress (0.2-percent offset) with temperature for the tensile stress-strain tests at constant temperature is also shown in figure 14 by the test points and dashed curve. This curve is a fair approximation of the results obtained for a temperature rate of 0.2° F per second. At higher rates, however, the yield stress for the rapid-heating test is substantially higher than the yield stress obtained in the stress-strain test under constant-temperature conditions. For a rate of 100° F per second, for example, the former is over 30 percent greater than the latter at 400° F. The increase in yield stress with temperature rates for a given temperature becomes fairly small at rates above 60° F per second.

Yield stresses for 2024-T3 are shown in figure 15 for temperature rates from 0.2° F to 100° F per second. The curves of figure 15 were prepared with the aid of the experimental curves of figure 13. The variation of the yield stress (0.2-percent offset) with temperature for the stress-strain tests at constant temperature is also shown for comparative purposes in figure 15 by the test points and dashed curve. In general, the yield stress under rapid-heating conditions increases with an increase in temperature rates except at 50 ksi and 300° F where it is more or less independent of rate. The increase in yield stress due to a rate of 100° F per second over the yield stress obtained in the stress-strain test at 600° F is about 60 percent; the corresponding increase at 400° F, however, is only about 3 percent. The yield stress for a temperature rate of 0.2° F per second falls somewhat below the yield stress for the stress-strain test over most of the range. As in the case of 7075-T6, the increase in yield stress with an increase in the temperature rate for a given temperature becomes fairly small at rates above 60° F per second. The correspondence between the yield stresses under rapid-heating conditions and those obtained in the stress-strain tests are markedly affected by the aging characteristics of this material, which affect both the rapid-heating and stress-strain results from about 250° F to 450° F.

Rupture Temperatures and Stresses

The variation of rupture temperature with temperature rate, plotted on a logarithmic scale, is shown in figures 16 and 17 for 7075-T6 and 2024-T3, respectively, for the various stress levels. Rupture temperatures, like yield temperatures, increase with increases in temperature rate. Considerably more scatter is evident, however, in the results for rupture temperatures than in the results for yield temperatures. (Compare figs. 16 and 12 for 7075-T6 and figs. 17 and 13 for 2024-T3.) More scatter can be expected for rupture temperatures because of the inherent variations in specimen and temperature conditions at rupture or fracture. The experimental curves for 7075-T6 (fig. 16) are fairly linear so that rupture temperatures are also approximately proportional to the logarithm of the temperature rate. The experimental curves for 2024-T3 (fig. 17) are only roughly linear and start to level off at 40 ksi. Rupture temperatures are therefore only roughly proportional to the logarithm of the temperature rate for this material.

Rupture stresses, defined as those stresses at which rupture temperatures occur under rapid-heating conditions, are shown in figure 18 for 7075-T6 for temperature rates of 0.2°, 2°, 20°, 60°, and 100° F per second. Rupture temperatures for these heating rates were determined from the experimental curves in figure 16. The variation of the ultimate stress obtained from the stress-strain tests at constant temperature and 1/2-hour exposure is also shown in figure 18 by the test points and dashed

curve. Rupture stresses at temperature rates of 100° F per second are substantially greater at a given temperature than ultimate stresses obtained from stress-strain tests under constant-temperature conditions. Even at a temperature rate of 0.2° F per second, the rupture stresses are somewhat greater over the entire temperature range than ultimate stresses obtained from stress-strain tests. Rupture temperatures are only on the order of 20° F to 30° F higher than yield temperatures for 7075-T6 for corresponding stress levels and temperature rates. (Compare figs. 18 and 14.)

Rupture stresses for 2024-T3 are shown in figure 19 for temperature rates from 0.2° F to 100° F per second. Rupture temperatures for this figure were determined from the experimental curves of figure 17. The variation of the ultimate stress obtained from the stress-strain tests under constant-temperature conditions is also shown in figure 19. At 100° F per second, rupture stresses are substantially higher at a given temperature above 500° F than ultimate stresses obtained from stress-strain tests. The increase in rupture stress with temperature rates for a given temperature becomes fairly small at rates above 60° F per second. Rupture temperatures for 2024-T3 are about 30° F to 60° F higher at the same stress level and temperature rate than corresponding yield temperatures (fig. 15), about twice as great a difference as found for 7075-T6.

Fracture

Typical fractures are shown in figure 20 for specimens of 2024-T3 and 7075-T6. The specimens in each group are arranged in the order of increasing stress from top to bottom. Elongations and types of fracture are given in tables 2 and 3 for 7075-T6 and 2024-T3, respectively.

The type of fracture varies with the stress level and temperature. For very low stresses at which high temperatures are reached, the fracture is a brittle, ragged, right-angle type of break (top specimens of each group, fig. 20). At intermediate stresses and temperatures, considerable necking is apparent (intermediate specimens of each group), and the fracture is more or less normal to the surface with some indications of shearing. At high stresses and correspondingly low temperatures, shear-type failures occur at an angle of approximately 45° to the surface (last specimens of each group).

TEMPERATURE-RATE PARAMETERS AND APPLICATION

Linear Temperature Parameter

Examination of the yield- and rupture-temperature results for 7075-T6 (figs. 12 and 16) indicates that approximately linear experimental relations

may be obtained between these temperatures and the logarithm of the temperature rate for the various stress levels. Further examination of the yield-temperature results on an enlarged scale shows that each stress level can be closely approximated by straight lines which intersect at a single point (fig. 21). If this point is denoted by the temperature and temperature-rate constants T_a and h_a, respectively, the slopes m of the curves can be given as

$$\frac{T - T_a}{\log h - \log h_a} = m \tag{1}$$

where T and T_a are temperatures in $^{\circ}F$, and h and h_a are temperature rates in $^{\circ}F$ per second.

In equation (1), $\frac{T - T_a}{\log h - \log h_a}$ is a parameter which is a function of stress. Consequently, plots of stress against this parameter should yield a single curve. The parameter therefore takes into account the effect of both temperature and temperature rate at different stress levels. Inasmuch as $T_a = -200^{\circ}$ F and $\log h_a = -17$ (fig. 21), the yield parameter for 7075-T6 becomes

$$\frac{T + 200}{\log h + 17} \tag{2}$$

Parameter (2) is found to hold for rupture as well as for yield temperature for this material, so that T applies either to yield or rupture temperature. This parameter is of the same form as the linear time-temperature parameter of Manson and Haferd (ref. 8), which has been applied to creep tests, the difference being the substitution of the temperature rate for the minimum creep rate in this parameter.

Even though the assumption of linearity of yield and rupture temperatures with the logarithm of the temperature rate is questionable at some stress levels for 2024-T3 (figs. 13 and 17), an attempt was made to see whether a rate parameter could be derived for this material which might prove useful in estimating or predicting the effects of different temperature rates. Only a rough approximation of the yield temperatures by straight lines intersecting at a point was found to be possible for this material (fig. 22). On the basis of the assumed straight lines, the parameter for yield temperatures for 2024-T3 is

$$\frac{T + 200}{\log h + 19} \tag{3}$$

Parameter (3) is found to be valid for rupture as well as for yield temperatures for 2024-T3; T applies to both yield and rupture temperatures.

Reciprocal Temperature Parameter

A reciprocal temperature parameter was also derived for 7075-T6 and 2024-T3. This parameter was based upon an observed linearity of plots of the reciprocal yield temperature against the logarithm of the temperature rate at constant stress and the tendency for such lines to converge to a single point at zero reciprocal temperature. This parameter is

$$T(24 - \log h) \tag{4}$$

where T is the absolute temperature in $^{\circ}R$ and h is the temperature rate in $^{\circ}F$ per second. Parameter (4) gives equivalent combinations of temperature and temperature rate for given stress levels and can be used to construct master curves of stress against the parameter for yield and rupture temperatures of both 7075-T6 and 2024-T3. This parameter is of the same form as the Larson and Miller parameter (ref. 9).

Master Yield and Rupture Curves

Master curves for 7075-T6.- Master yield and rupture curves for 7075-T6 employing the linear temperature parameter (2) are shown in figure 23. Good correlation was found particularly for yield temperatures at 40 ksi and 60 ksi where the test points are closely superimposed. The correlation for rupture temperatures is fairly good except at 40 ksi where the scatter of the data is considerable.

The master curves for yield and rupture are linear from about 17 ksi to 65 ksi. The yield stress σ_y, which corresponds to the yield temperature T_y, may be expressed as

$$\sigma_y = 133.5 - 2.55\left(\frac{T_y + 200}{\log h + 17}\right) \tag{5}$$

The rupture stress σ_r at which the rupture temperature T_r occurs may be given as

$$\sigma_r = 143.5 - 2.69\left(\frac{T_r + 200}{\log h + 17}\right) \tag{6}$$

In equations (5) and (6), the stresses σ_y and σ_r are in ksi, the temperatures T_y and T_r are in °F, and the temperature rate h is in °F per second. These formulas are limited to stresses from 17 ksi to 65 ksi.

The correlation of the data for yield and rupture temperatures employing the reciprocal temperature parameter (4) was almost identical with that obtained with the linear parameter (2). Consequently, the master curves based on the reciprocal parameter are not included.

The validity of the linear parameter is shown by the correlation of the data with the master curves (fig. 23). A more critical evaluation of the accuracy obtainable by the use of the master curve and the parameter may be had by making a comparison of predicted or calculated yield and rupture temperatures with the test results at different stress levels. Calculated yield temperatures (fig. 12) agree within 10° F with the test results. Calculated rupture temperatures (fig. 16) are also in close agreement with the test results except at 40 ksi where there is a maximum difference of about 20° F. Similar calculations, based upon the master curves, using the reciprocal temperature parameter (4) were in very close agreement with those shown in figures 12 and 16.

Master curves for 2024-T3.- Master yield and rupture curves for 2024-T3 using the linear temperature parameter (3) are shown in figure 24. The correlation of the data is not so good for this material as that obtained for 7075-T6 (fig. 23). The correlation is very poor at 50 ksi for yield temperatures and only fair at 40 ksi for rupture temperatures.

The master curves for yield and rupture can be assumed to be linear over part of the range. The yield stress σ_y under rapid-heating conditions can be given as

$$\sigma_y = 106.0 - 2.03\left(\frac{T_y + 200}{\log h + 19}\right) \tag{7}$$

The rupture stress σ_r can be expressed as

$$\sigma_r = 127.5 - 2.38\left(\frac{T_r + 200}{\log h + 19}\right) \tag{8}$$

In equations (7) and (8), the stresses σ_y and σ_r are in ksi, the temperatures T_y and T_r are in °F, and the temperature rate h is

in °F per second. Equations (7) and (8) are limited, respectively, to the 16-ksi to 40-ksi and 16-ksi to 50-ksi ranges.

As in the case of 7075-T6, the correlation of the data for yield and rupture employing the reciprocal temperature parameter (4) was practically the same as that obtained with the linear temperature parameter (2). Master curves based on the former are therefore not included.

Calculated yield and rupture temperatures based upon the use of the linear temperature parameter are compared with the test results in figures 13 and 17. Fair agreement is obtained except at 50 ksi for yield temperatures and at 40 ksi for rupture temperatures. The agreement between calculated and experimental results, however, is not so good for this material as that for 7075-T6 (figs. 12 and 16). It is not surprising that the same parameters do not work so well for 2024-T3 as for 7075-T6 because aging of the former markedly alters the general pattern of the results. Calculated yield and rupture temperatures, obtained by means of the reciprocal temperature parameter (4), were in close agreement with those shown for the linear temperature parameter (3).

CONCLUDING REMARKS

In the rapid-heating tensile tests of 7075-T6 and 2024-T3 aluminum-alloy sheet under constant load and temperature rates from 0.2° F to 100° F per second, yield and rupture temperatures were found to increase approximately in proportion to the logarithm of the temperature rate except in certain regions for 2024-T3 aluminum alloy where aging affected the results.

Under rapid-heating conditions, yield and rupture stresses may be substantially greater or about the same for a given temperature as corresponding stresses obtained from elevated-temperature tensile stress-strain tests for 1/2-hour exposure, depending upon the temperature rate and material. The increase in yield and rupture stresses with temperature rates for a given temperature becomes fairly small at rates above 60° F per second.

Linear and reciprocal temperature-rate parameters made it possible to take into account the effect of the temperature rate and to construct single or master curves of stress against the parameter. These curves provide a convenient method of obtaining yield and rupture stresses and

temperatures for a given temperature rate. Good correlation of the data with the master curves was obtained except where aging altered the results.

Langley Aeronautical Laboratory,
National Advisory Committee for Aeronautics,
Langley Field, Va., March 25, 1955.

APPENDIX

DESCRIPTION OF TEST EQUIPMENT FOR RAPID-HEATING TESTS

Loading Equipment

The general arrangement of the loading equipment is shown in figure 2. The load was applied to the specimen through a 5:1 beam or lever system by means of weights. The fulcrum of the beam was supported on a plate mounted near the top of the three columns of a 120,000-pound-capacity two-way hydraulic jack. The weight-loading system had a maximum capacity of 10,000 pounds on the specimen. Knife edges were employed at the fulcrum and other loading points of the beam. With this system, the beam could be positioned and the weight cage could be lifted from the floor by lowering the ram of the two-way jack.

The method of connecting the specimen to the loading system is shown in more detail in figure 3. The load was applied to the specimen by means of yoke-and-pin connections. In order to prevent grounding at the top and bottom of the specimen, which was part of the electrical circuit, the loading bars were electrically insulated from the rest of the system. This insulation was provided by the two-piece rectangular load insulators shown above the top column plate and above the ram.

Because a discontinuity of slope was obtained in the time-temperature records at the beginning of heating, the possibility of inertia effects in the load system was investigated. Load variations were measured by means of a calibration bar in series with the specimen. The variation in output of two wire strain gages mounted on the bar was measured with a pen-type recorder with a 100-cycle-per-second response. No detectable variations in load occurred within the range of temperature rate covered by the tests. Small load oscillations were obtained, however, at rates above 150° F per second.

Strain-Measuring Equipment

The extensometer system consisted of two pairs of extensometer frames mounted opposite each other and 1 inch apart, and two strain-transfer units, each of which actuated a variable linear differential transformer-type gage. Details of the extensometer frames and contact ends of the strain-transfer units are shown in figure 4.

Each extensometer frame was made with a double-edge knife edge and a wire arm serving as a stabilizer for the knife edge and keeping it normal to the specimen surface. Spring clips were used to hold the knife

edges in firm contact with the specimen surface and were mounted in such a manner as to keep the frictional forces at the ends of the arms at a minimum in order to avoid knife-edge slippage. Commercial lava blocks were mounted at the ends of the arms so as to insulate the arms from the specimen and prevent possible burning of the knife edges during heating and at rupture. The globular material visible at the ends of the frames (fig. 4) consisted of a ceramic cement which held the lava blocks securely to the wire arms. The frames were mounted and spaced 1 inch apart on the specimen by means of a gage block.

The strain-transfer units were mounted independently of and at right angles to the specimen so as to keep the effect of temperature on the strain-transfer unit and the differential transformer at a minimum (figs. 3 and 4). The tubular arms of the strain-transfer units were mounted on flexure plates about at their midposition. A vertical displacement of the specimen with respect to the strain-transfer units did not result in an indicated strain except for slight variations due to extensometer-contact irregularities and small angularity effects. The output of the two gages was added so that an average value of strain was obtained. Each end of each strain-transfer arm was in point contact with the flat horizontal surface of one of the knife-edge units (fig. 4). The arms were weighted in such a manner that positive contact was maintained throughout the test. In order to avoid damage to the knife edges and strain-transfer units under rupture conditions, end pieces supporting the contact points were attached magnetically to the ends of the tubular arms of the strain-transfer units. Release of the joint occurred only if more than the normal contact pressure was exerted. The contact points were insulated electrically from the end pieces.

Heating Equipment

Heating was accomplished by passing a high-amperage low-voltage alternating current directly through the specimen. Continuous voltage control was achieved by means of a 400-volt induction voltage regulator which was used to regulate manually the primary voltage of a 75-kilovolt-ampere transformer having an output of 3.8 to 20 volts. The transformer and regulator can be seen mounted on the wooden stand in figure 2.

Two connections, one on each side of the specimen, were used between each end of the specimen and the bus bars from the transformer. Each connection consisted of five thin, flexible braided copper leads silver-soldered together to form a flat terminal which provided a good electrical contact with the specimen surfaces. These flexible leads were clamped to the specimen with small clamps at one end, and each lead was bolted to the bus bars at the other end.

Temperature-Measuring Equipment

Temperatures were measured with No. 28 gage chromel-alumel thermocouples which were flattened and held in firm contact with the specimen surface by means of special mountings and clamps. The thermocouple junction was fused by means of a mercury arc. Two thermocouples were located at the midposition directly opposite each other on the faces of the specimen so as to provide a check on the temperature measurements in the region in which the strains were measured. Single thermocouples were also clamped at points 3 inches above and below the midposition to provide information on the temperature gradient. Two recording potentiometers, each having two channels, were used and had response rates of full-scale travel in 1 second. Inasmuch as one channel was required for strain measurements, three of the four available channels were used for temperature measurements. Four temperatures were recorded on three channels by alternately switching manually the output of the upper and lower thermocouples to the input of a single channel during the test.

The method of clamping the two thermocouples at the midposition is illustrated in figure 5. Each thermocouple was held in positive contact with the specimen surface by an asbestos pad cemented to a thin backing plate, an extension of which held the thermocouple in a fixed position on the asbestos pad. The backing plate consisted of a flattened portion of thin Inconel tubing. The pad insulated the thermocouple from the air and the backing plate. An adjustable clamp provided the pressure necessary to insure reliable temperature indications. This method of clamping thermocouples has proved to be quick and convenient. Consistent results are possible for the aluminum-alloy specimens with this arrangement if intimate contact of the flattened thermocouple and specimen surface is obtained, the asbestos pad is in good condition, and adequate pressure is applied. Thermocouples mounted in this manner can be used repeatedly.

In order to determine whether the results obtained with clamped thermocouples were consistent with those obtained from thermocouples peened into small holes in the surface, comparisons were made between two clamped and one peened thermocouple located at the same height on the specimen for a temperature rate of 100° F per second. The comparisons showed that the maximum variation in response rate between the two types of thermocouples was about 3/4 percent. The scatter at 800° F at the same instant was about 5° F for the two clamped thermocouples. Temperatures measured by the peened thermocouple fell between those obtained for the clamped thermocouples. Indicated temperatures obtained with the two clamped thermocouples generally agreed within a few degrees. If the installation was imperfect, however, low or inconsistent temperatures were obtained from either peened or clamped thermocouples.

Specimen Temperature Gradients

Typical temperature gradients obtained along the length of the reduced section of the rapid-heating specimen for temperature rates of 2° F and 110° F per second are shown in figure 6 for center temperatures of 400° F to 500° F. Temperatures were measured at the positions shown by means of peened thermocouples and an oscillograph recorder having 18 channels. In order to duplicate test conditions, the measurements were taken with the specimen mounted in position for testing and with the extensometer frames and clamped thermocouples in place. The results show the marked effect of the extensometer frames and clamped thermocouples on the local temperature distribution. The normal gradient without equipment mounted on the specimen is a smooth curve which is concave toward the specimen. The addition of the extensometer and clamped thermocouples depresses the normal curve as the result shows. The temperature variation within the 1-inch gage length is fairly uniform for 2° F per second but varies about 10° F for the 110° F rate at a temperature of 400° F to 500° F. At higher temperatures, this variation would be somewhat greater and at lower temperatures, somewhat less. The effect of the clamped thermocouple 3 inches from the center line in reducing temperatures shows up clearly at 110° F per second. Because of the cooling effect of the extensometer, temperatures just outside the gage length were 20° F to 30° F higher than those inside the 1-inch-gage-length region at this temperature. Rupture of the specimens therefore usually occurred just outside the gage length. Because temperatures at rupture were measured by thermocouples at the center line of the specimen, rupture temperatures are somewhat conservative.

The adverse effects of mounting thermocouples and extensometer frames in this manner are considerably alleviated by the use of comparatively thick specimens of good conductor materials such as aluminum. In preliminary tests of thin titanium-alloy sheet, however, temperature variations in the gage length were much more pronounced because of the relatively poor conductivity of the specimens. Consequently, the extensometer frames were redesigned to provide less point-contact area, and very small peened thermocouples were employed.

REFERENCES

1. Cross, H. C., McMaster, R. C., Simmons, W. F., and VanEcho, J. A.: Short-Time, High-Temperature Properties of Heat-Resisting Alloy Sheet. Project RAND (USAF Project MX-791) RA-15077, Douglas Aircraft Co., Inc., Feb. 27, 1948.

2. Smith, W. K., Wetmore, W. O., and Woolsey, C. C., Jr.: Tensile Properties of Metals While Being Heated at High Rates. NAVORD Rep. 1178, Pt. 1 (NOTS 234), U. S. Naval Ord. Test Station (Inyokern, Calif.), Sept. 7, 1949.

3. Smith, W. K., Woolsey, C. C., Jr., and Wetmore, W. O.: Tensile Properties of Metals While Being Heated at High Rates. Pt. 2 - Aluminum Alloys. NAVORD Rep. 1178 (NOTS 319), U. S. Naval Ord. Test Staion, Inyokern (China Lake, Calif.), Sept. 1, 1950.

4. Smith, W. K., Woolsey, C. C., Jr., and Wetmore, W. O.: Tensile Properties of Metals While Being Heated at High Rates. Pt. 3 - Comparison of Results From High-Heating-Rate Tests With Results From Rocket Firing Tests. NAVORD Rep. 1178 (NOTS 336), U. S. Naval Ord. Test Station, Inyokern (China Lake, Calif.), Dec. 20, 1950.

5. Smith, W. K.: High-Heating-Rate Strength of Titanium and Two Titanium Alloys. NAVORD Rep. 1958 (NOTS 526), U. S. Naval Ord. Test Staion, Inyokern (China Lake, Calif.), Apr. 10, 1952.

6. Miller, B. A., Winward, J. M., and Smith, W. K.: High-Heating-Rate Strength of Three Heat-Resistant Metals. NAVORD Rep. 2017 (NOTS 670), U. S. Naval Ord. Test Station, Inyokern (China Lake, Calif.), Mar. 16, 1953.

7. Hughes, Philip J., Inge, John E., and Prosser, Stanley B.: Tensile and Compressive Stress-Strain Properties of Some High-Strength Sheet Alloys at Elevated Temperatures. NACA TN 3315, 1954.

8. Manson, S. S., and Haferd, A. M.: A Linear Time-Temperature Relation for Extrapolation of Creep and Stress-Rupture Data. NACA TN 2890, 1953.

9. Larson, F. R., and Miller, James: A Time-Temperature Relationship for Rupture and Creep Stresses. Trans. A.S.M.E., vol. 74, no. 5, July 1952, pp. 765-771; Discussion, pp. 771-775.

TABLE 1

TENSILE STRESS-STRAIN PROPERTIES OF 0.125-INCH-THICK 7075-T6 AND 2024-T3 ALUMINUM-ALLOY SHEET FOR 1/2-HOUR EXPOSURE AND STRAIN RATE OF 0.002 PER MINUTE

Temperature, °F	Yield stress, ksi	Ultimate stress, ksi	Young's modulus, psi	Elongation in 2 inches, percent
7075-T6 aluminum-alloy sheet				
80	72.8	79.8	10.2×10^6	10
	74.8	80.0	10.4	12
200	67.6	71.2	9.9	16
	66.0	70.2	10.0	14
400	39.3	40.8	8.9	12
	40.4	41.8	8.9	13
600	8.6	9.0	6.0	34
	8.8	9.1	5.8	33
2024-T3 aluminum-alloy sheet				
80	51.4	70.2	10.2	22
	53.4	72.2	10.2	21
200	49.9	66.6	10.1	21
	50.6	66.4	10.1	20
400	45.9	57.2	9.5	10
	43.3	55.8	9.5	13
600	17.5	18.7	8.3	16
	17.6	19.1	8.1	18
688	8.0	9.2	7.2	24
710	7.1	8.5	7.8	23

TABLE 2

TENSILE PROPERTIES OF 7075-T6 ALUMINUM-ALLOY SHEET FOR TEMPERATURE RATES FROM 0.2° F TO 100° F PER SECOND

Stress, ksi	Temperature rate, °F/sec	Yield temperature, °F	Rupture temperature, °F	Elongation in 2 inches, percent	Type of fracture
0.4	0.233	---	---	--	Brittle
	60	---	---	--	Brittle
8	.233	633	680	37	Part brittle, part ductile
	58	764	820	--	Part brittle, part ductile
17.2	.233	542	567	17	Part brittle, part ductile
	2	590	615	14	Part brittle, part ductile
	15	633	653	18	Part brittle, part ductile
	60	658	690	20	Part brittle, part ductile
	96	665	---	11	Part brittle, part ductile
21.2	60	632	---	--	----------
40	.233	395	432	11	Ductile
	2	437	484	11	Ductile
	14	463	480	10	Ductile
	54	483	518	10	Part brittle, part ductile
	92	495	497	11	Part brittle, part ductile
56.3	15	353	390	11	Ductile
60	.233	273	308	12	Ductile
	2	300	351	12	Ductile
	15	323	358	--	Ductile
	58	345	376	--	Ductile
	91	351	391	11	Ductile
65	.2	262	319	28	Ductile

TABLE 3

TENSILE PROPERTIES OF 2024-T3 ALUMINUM-ALLOY SHEET FOR TEMPERATURE RATES FROM 0.2° F TO 100° F PER SECOND

Stress, ksi	Temperature rate, °F/sec	Yield temperature, °F	Rupture temperature, °F	Elongation in 2 inches, percent	Type of fracture
0.4	0.233	---	----	--	Brittle
	58	---	----	--	Brittle
8	.233	697	743	40	Brittle
	2	767	805	29	Brittle
	15	799	839	29	Brittle
	59	823	897	--	----------
	96	828	887	14	Brittle
16.5	.233	603	663	28	Part brittle, part ductile
	2	659	705	15	Part brittle, part ductile
	15	701	744	15	Part brittle, part ductile
	53	699	760	17	Part brittle, part ductile
	102	717	768	--	----------
28	2	550	604	--	----------
40	.233	403	504	5	Ductile
	2	426	537	12	Ductile
	14	454	----	--	----------
	57	---	[a]545	18	Ductile
	60	472	----	--	----------
	94	481	----	--	----------
	98	---	[a]555	18	Ductile
50	.233	297	399	8	Ductile
	2	279	440	12	Ductile
	15	305	447	13	Ductile
	61	304	467	--	Ductile
	99	297	478	12	Ductile

[a]Check tests for rupture.

TABLE 4

AVERAGE COEFFICIENTS OF THERMAL EXPANSION FOR

7075-T6 AND 2024-T3 ALUMINUM ALLOY

[Obtained from figs. 10 and 11 for 0.4 ksi]

Temperature, °F	Average coefficient of expansion per °F (a)					
	7075-T6			2024-T3		
	0.2° F/sec	60° F/sec	Stabilized	0.2° F/sec	60° F/sec	Stabilized
200	13.3×10^{-6}	13.3×10^{-6}	13.3×10^{-6}	13.2×10^{-6}	13.3×10^{-6}	13.2×10^{-6}
400	13.4	13.7	13.6	13.2	13.6	13.2
600	13.8	15.2	14.5	13.4	14.7	13.4
700	14.5	15.6	15.0	----------	----------	----------
800	----------	----------	----------	13.6	15.3	14.3

[a]Average value from 80° F to test temperature.

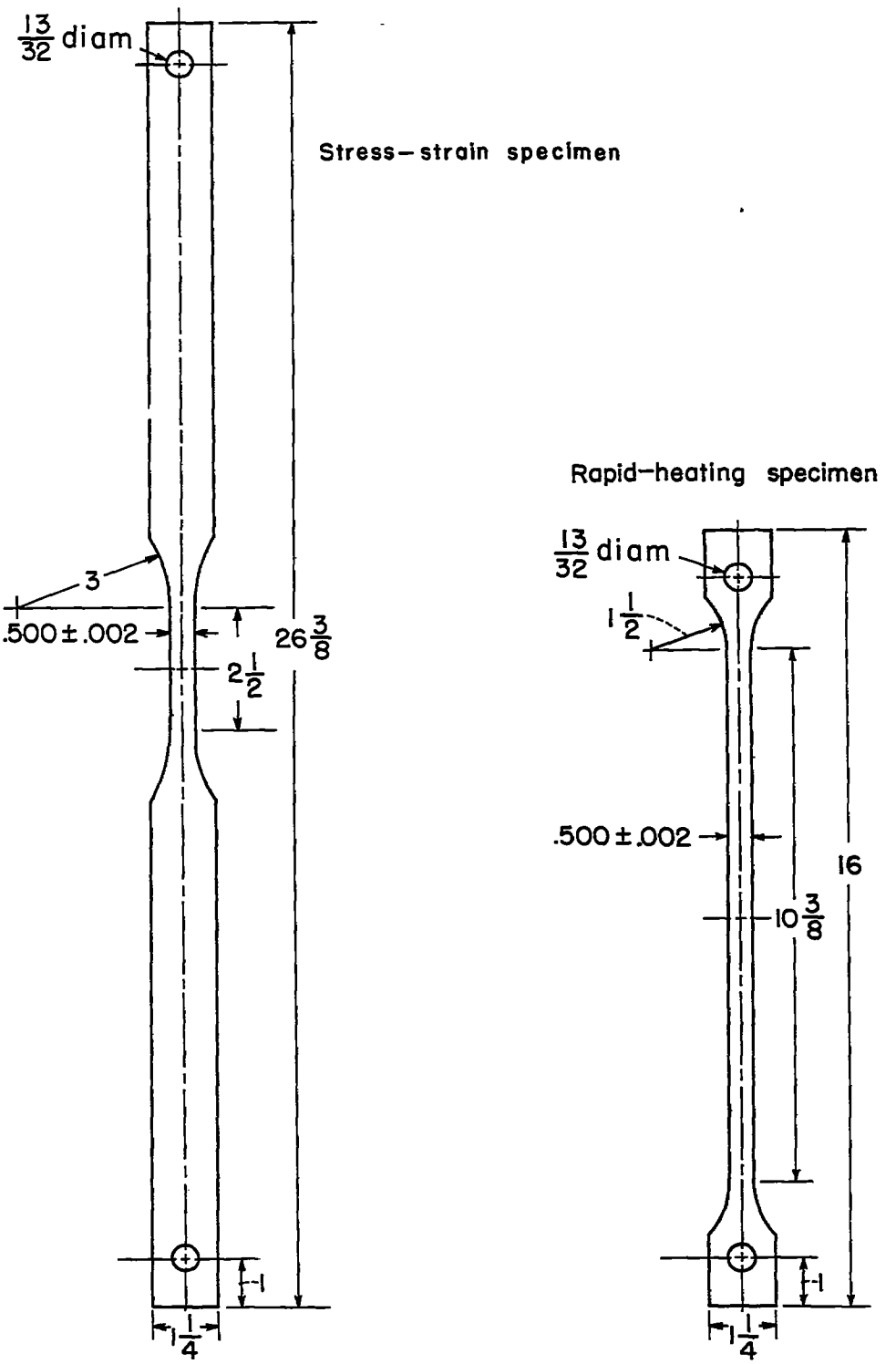

Figure 1.- Stress-strain and rapid-heating tensile test specimens. All dimensions are in inches.

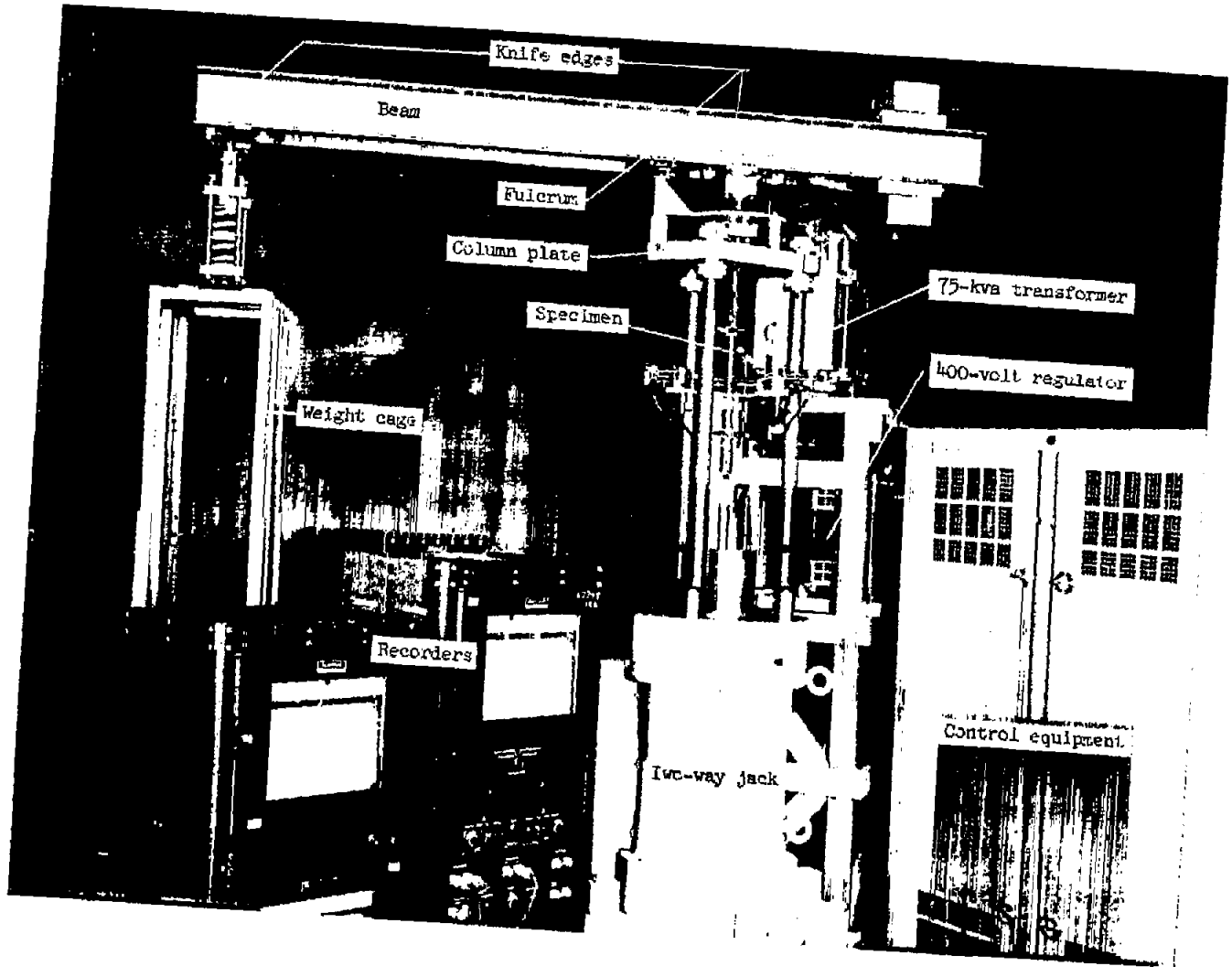

L-85860.1

Figure 2.- General arrangement of loading, heating, controlling, and recording equipment for rapid-heating tests.

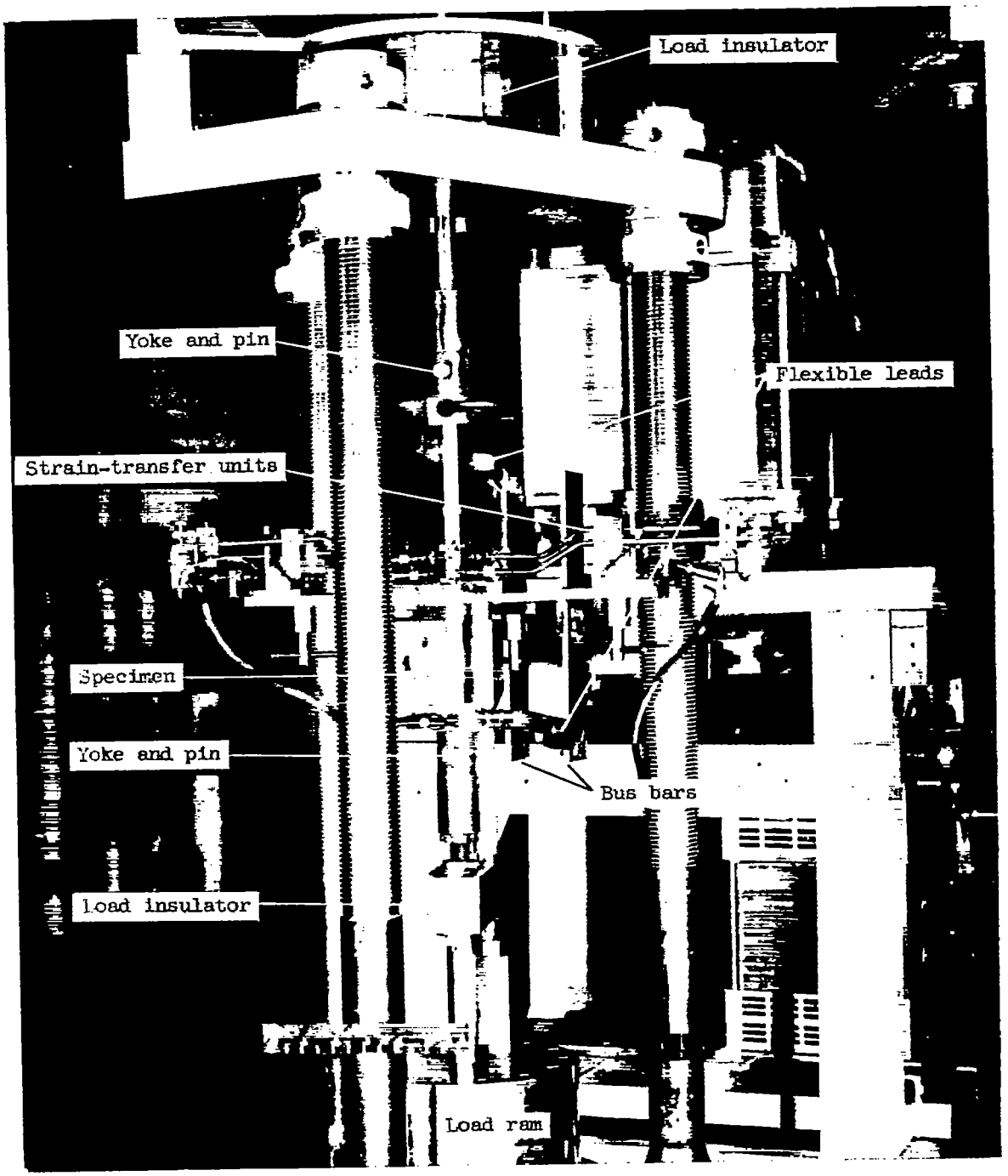

L-85861.1

Figure 3.- View of specimen mounted in position for testing.

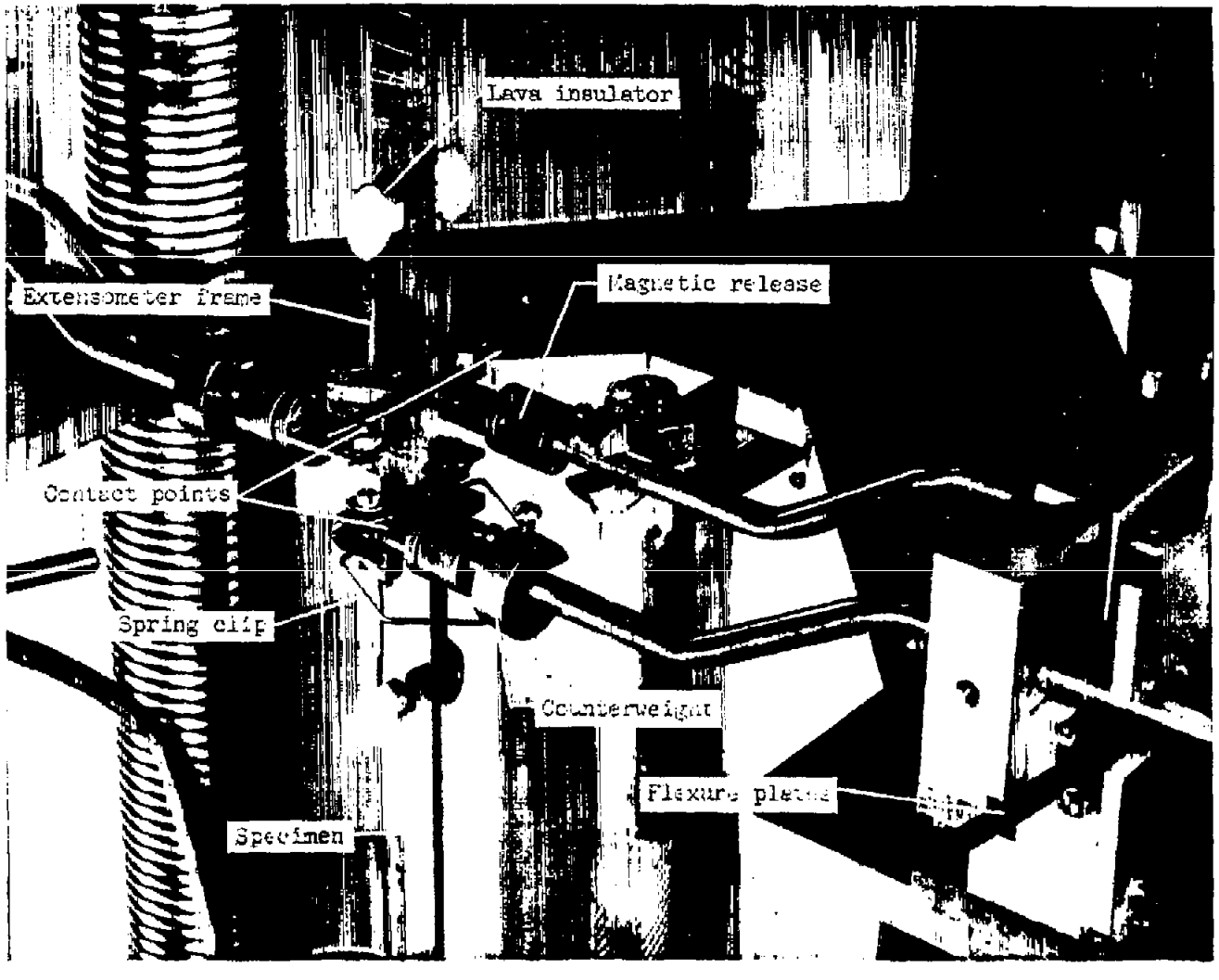

L-85198.1

Figure 4.- Details of extensometer system.

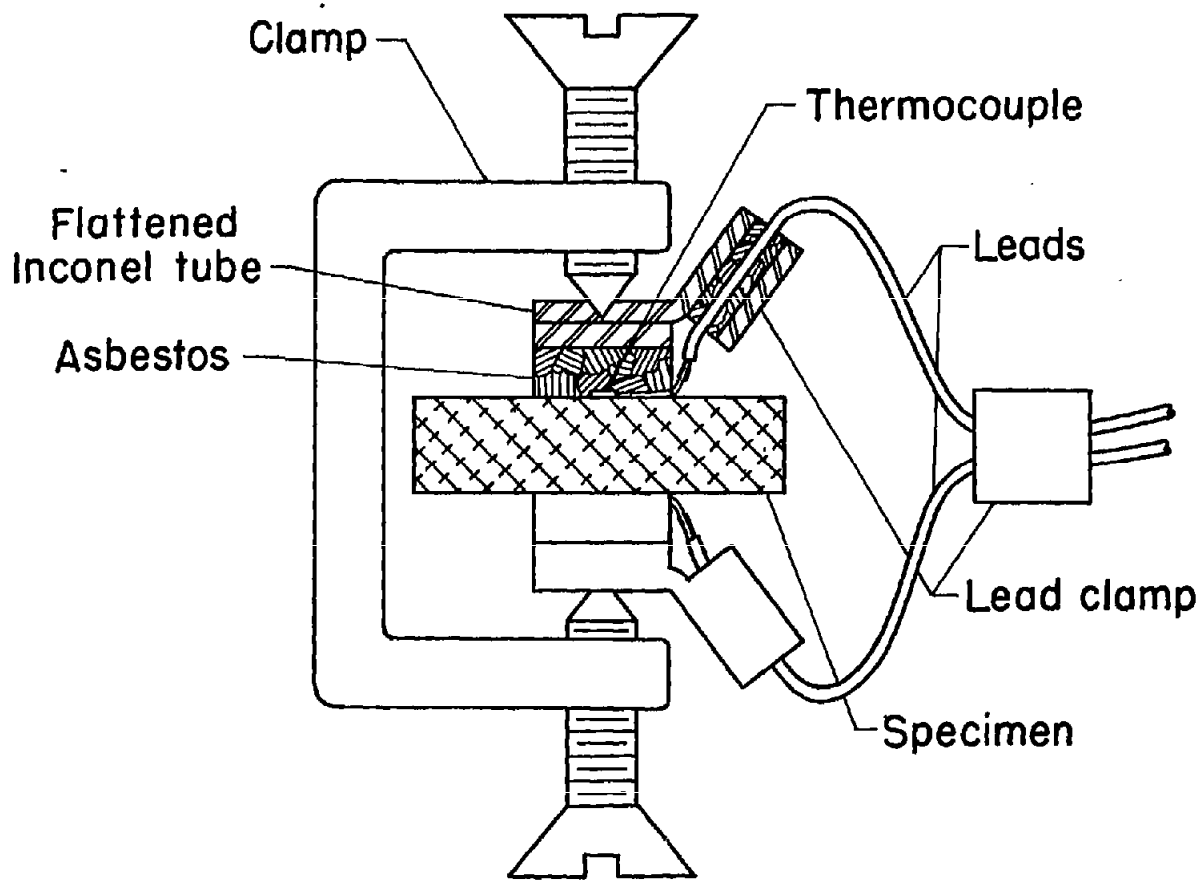

Figure 5.- Arrangement of specimen, thermocouple, and mounting clamp at midposition.

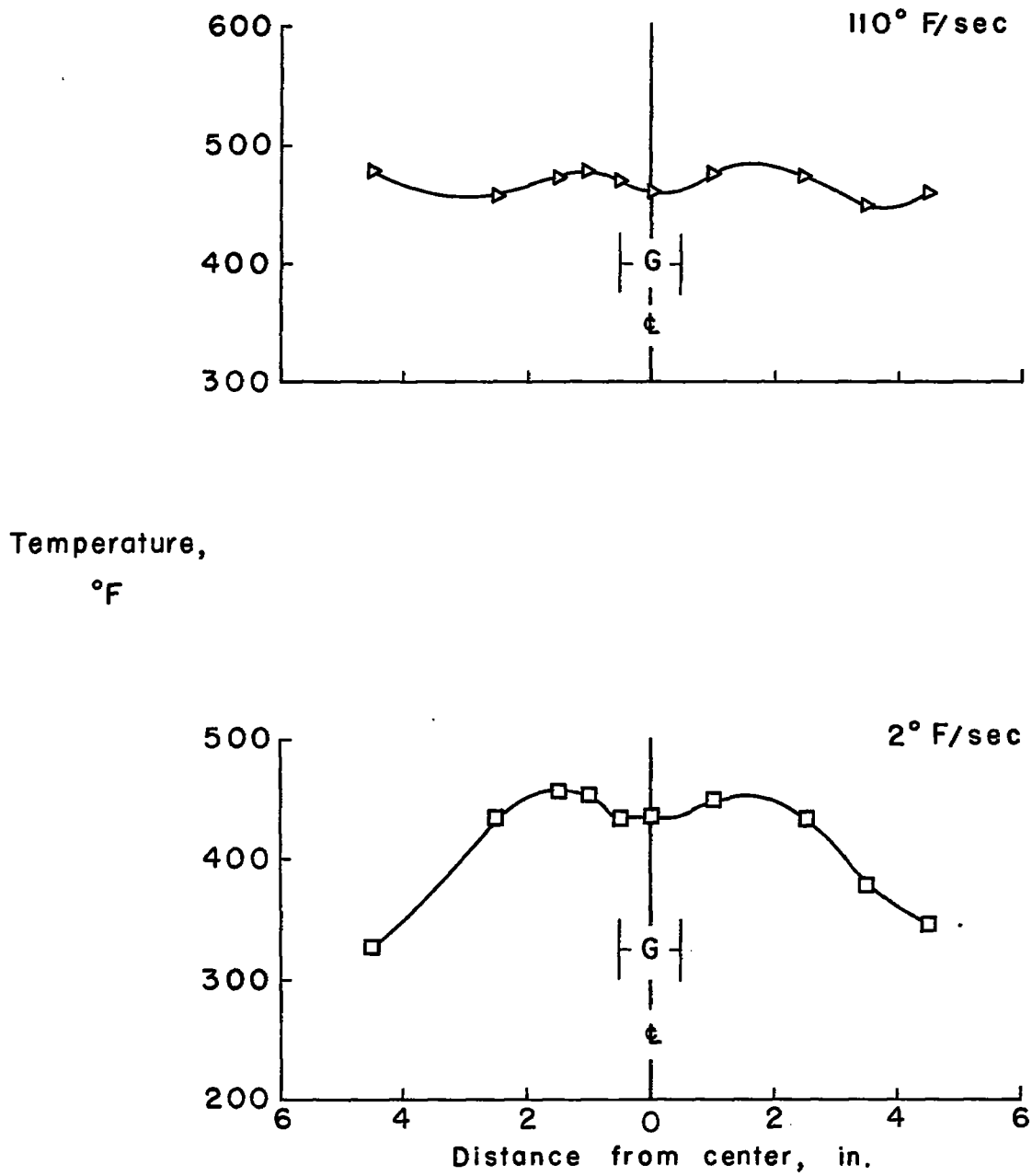

Figure 6.- Temperature gradients along length of rapid-heating specimen for temperature rates of 2° F and 110° F per second. Gage length is designated as G.

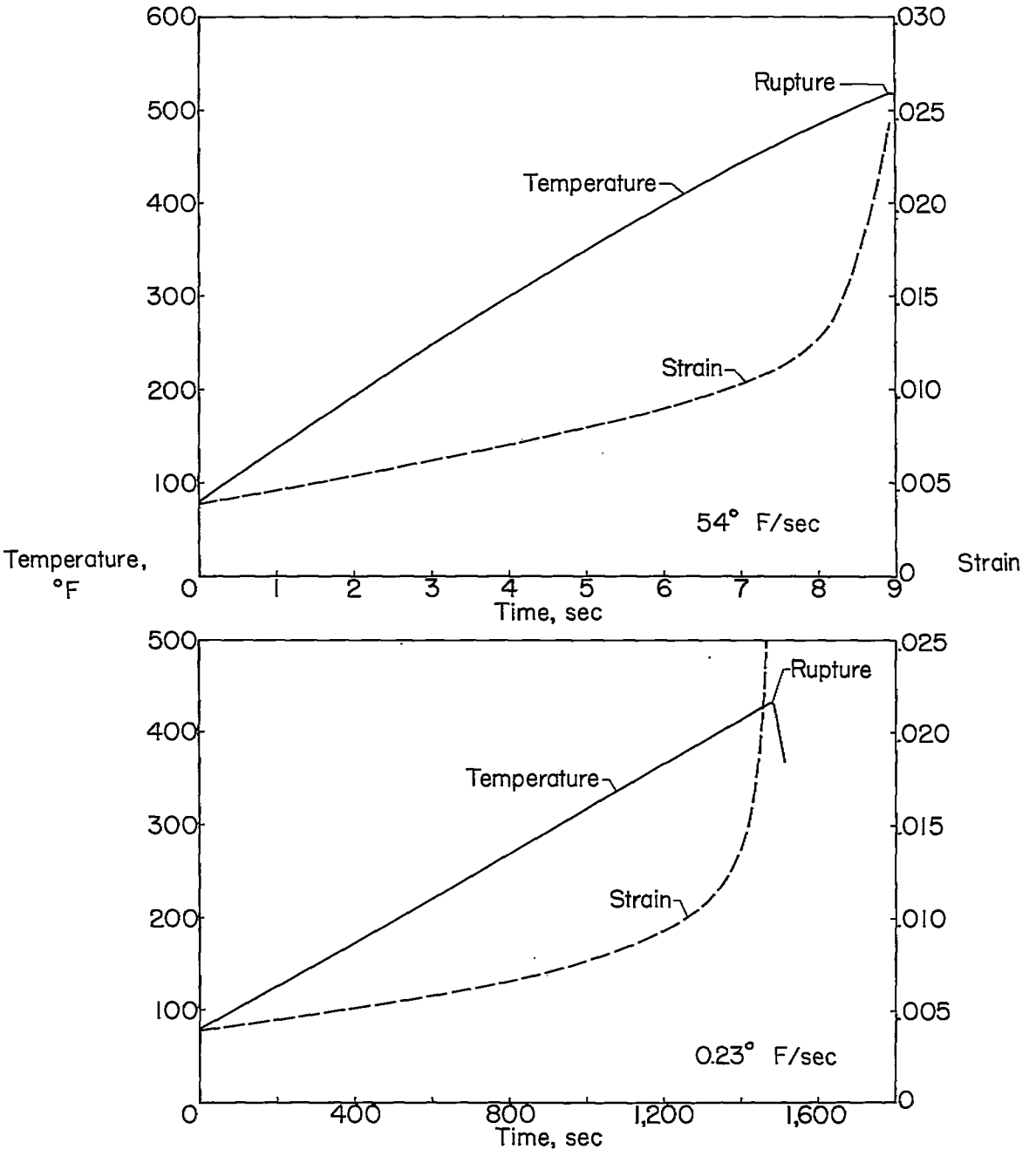

Figure 7.- Temperature- and strain-time curves for tests of 7075-T6 aluminum alloy at 54° F and 0.23° F per second at 40 ksi.

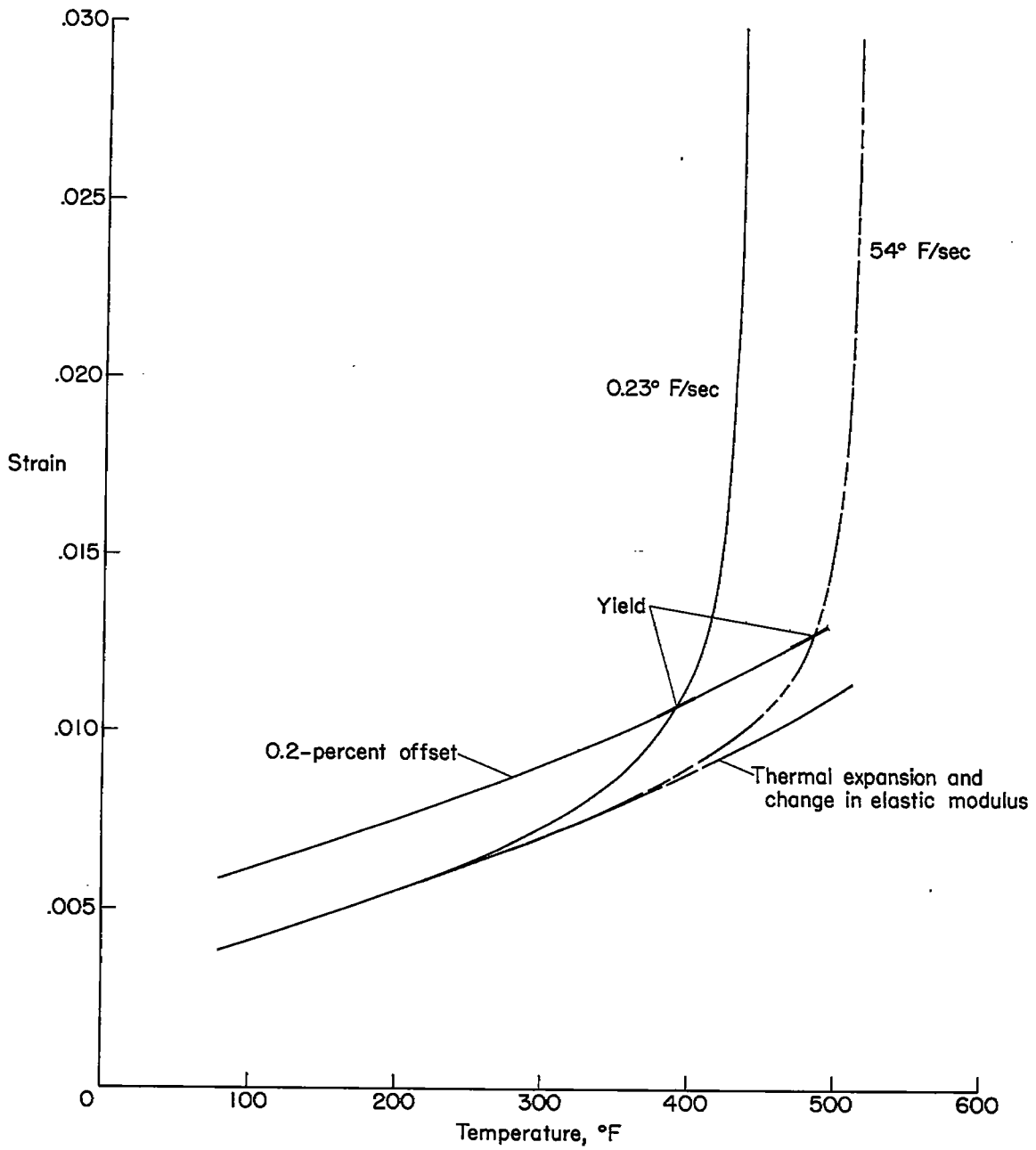

Figure 8.- Strain-temperature histories for tests at 54° F and 0.23° F per second for 7075-T6 aluminum alloy at 40 ksi.

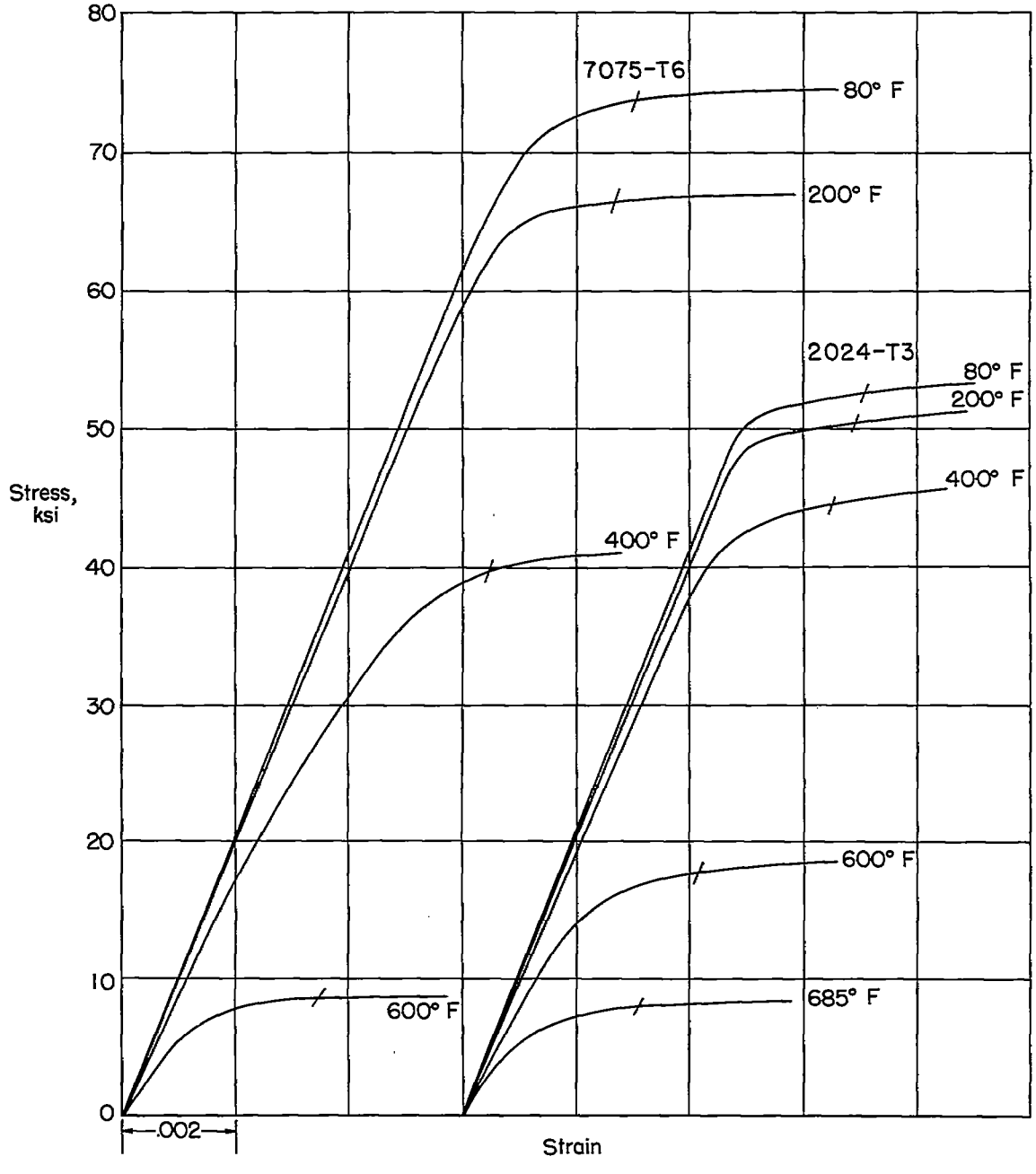

Figure 9.- Elevated-temperature tensile stress-strain curves for 7075-T6 and 2024-T3 aluminum-alloy sheet.

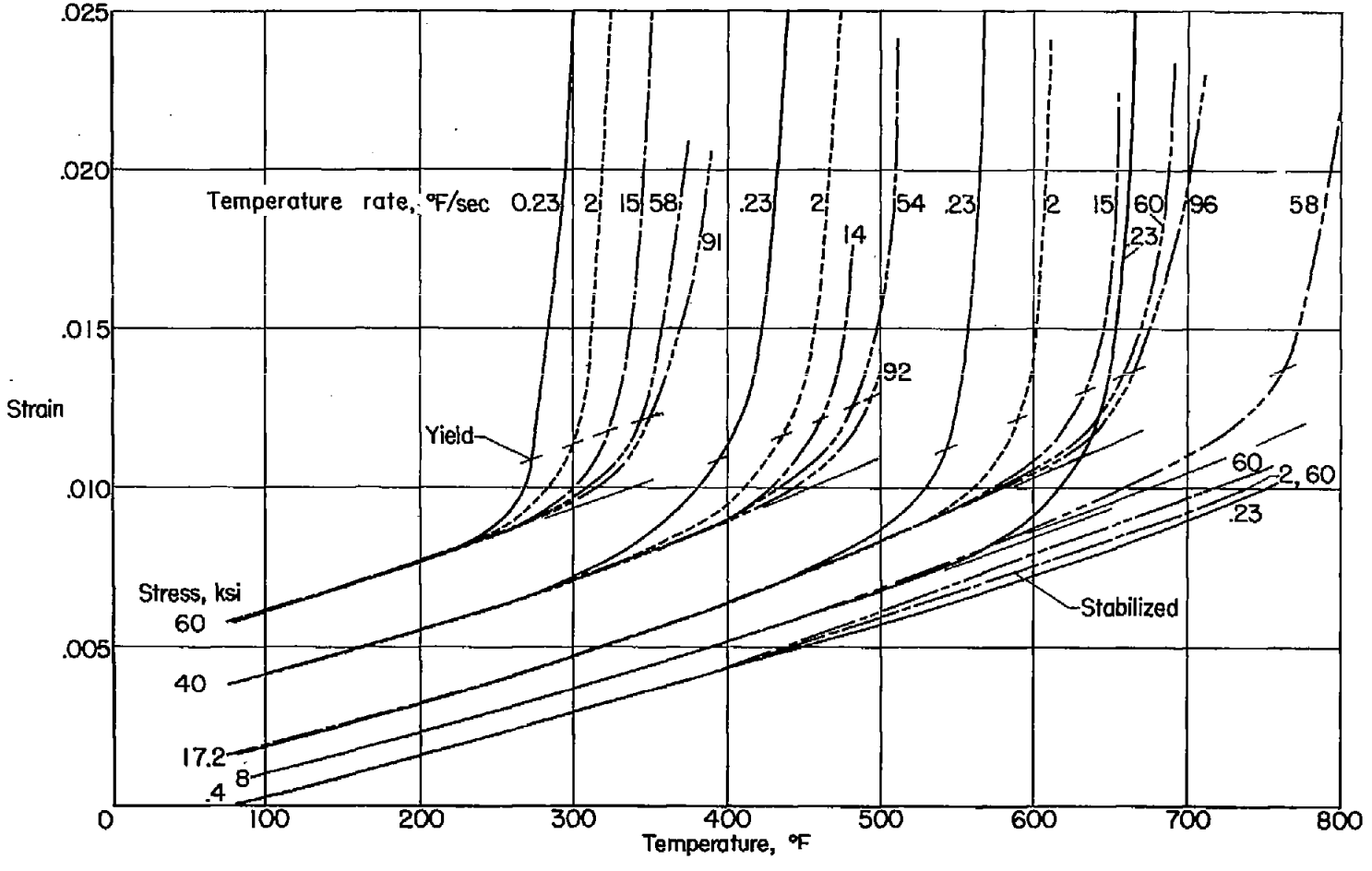

Figure 10.- Strain-temperature histories of 7075-T6 aluminum alloy for temperature rates from 0.2° F to 100° F per second for various stresses.

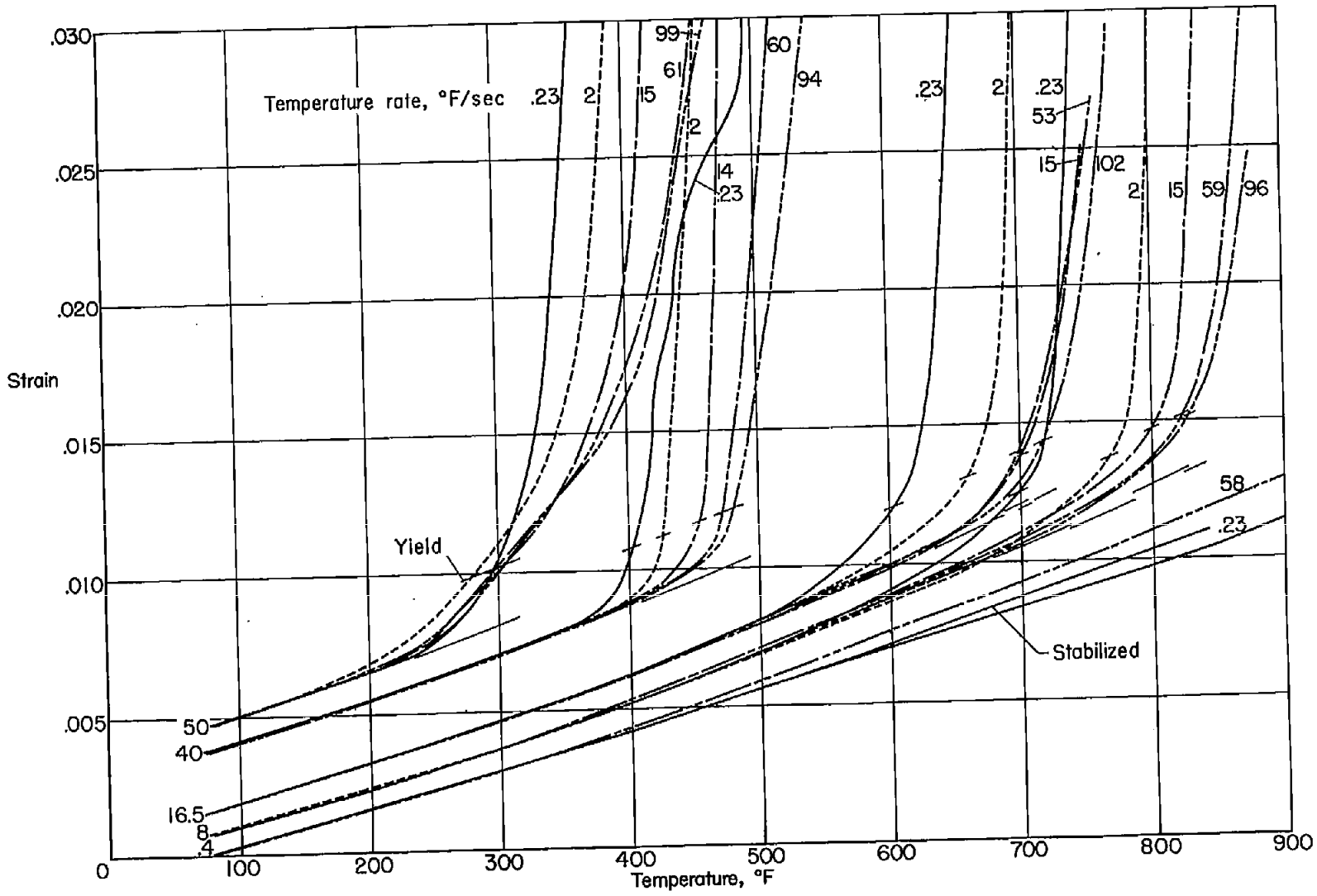

Figure 11.- Strain-temperature histories of 2024-T3 aluminum alloy for temperature rates from 0.2° F to 100° F per second for various stresses.

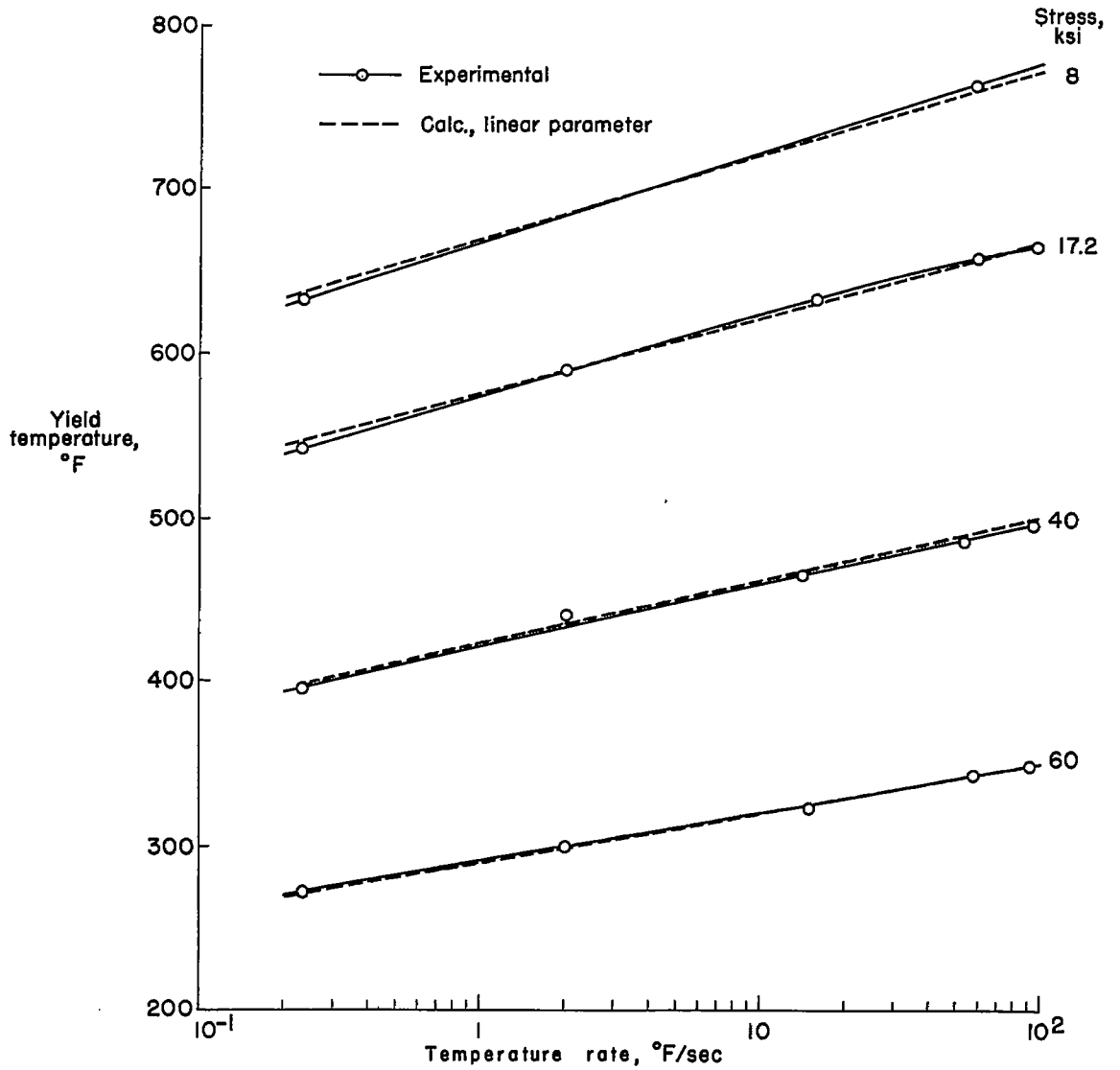

Figure 12.- Experimental and calculated yield temperatures of 7075-T6 aluminum alloy for temperature rates from 0.2° F to 100° F per second for various stresses.

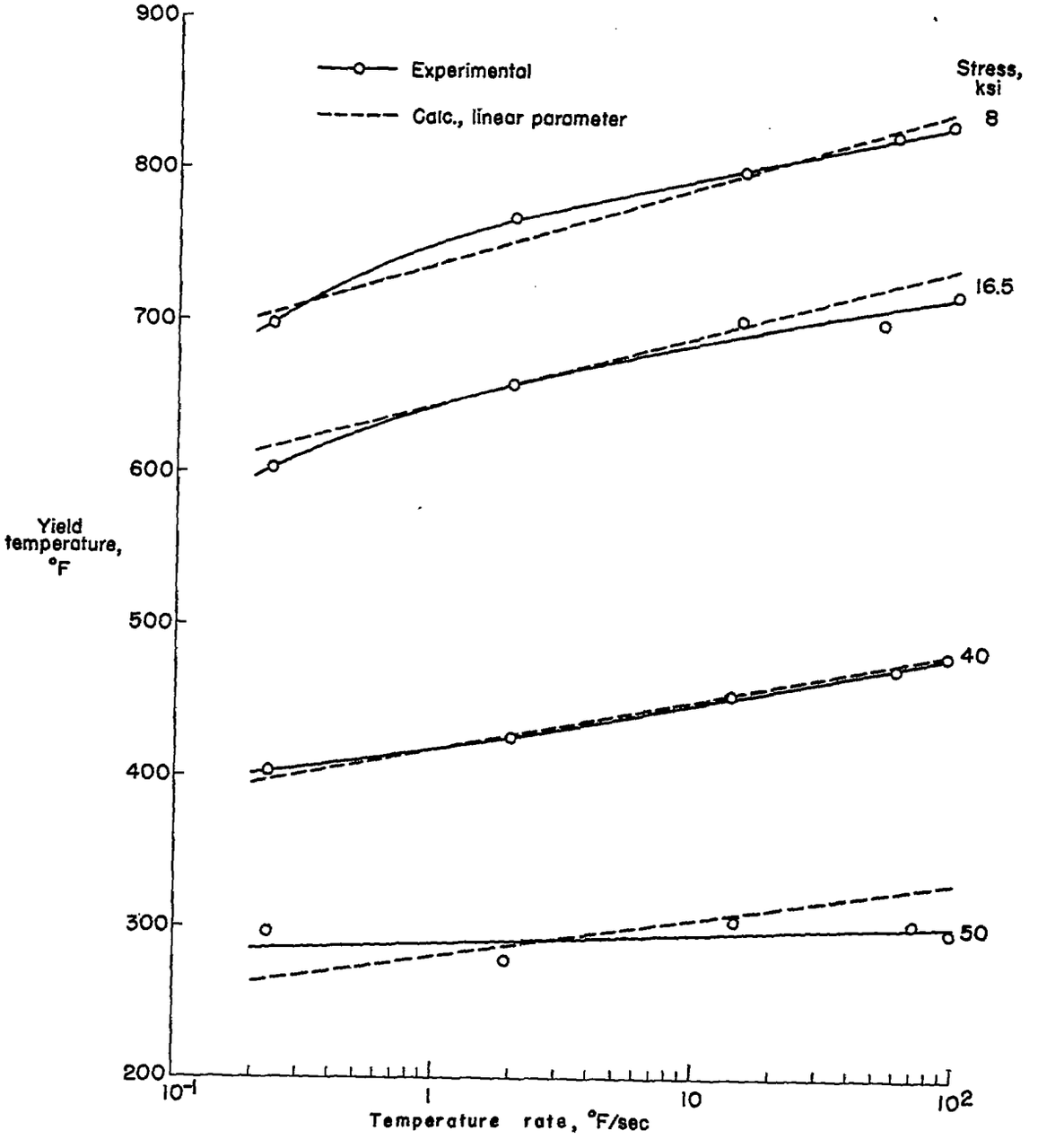

Figure 13.- Experimental and calculated yield temperatures of 2024-T3 aluminum alloy for temperature rates from 0.2° F to 100° F per second for various stresses.

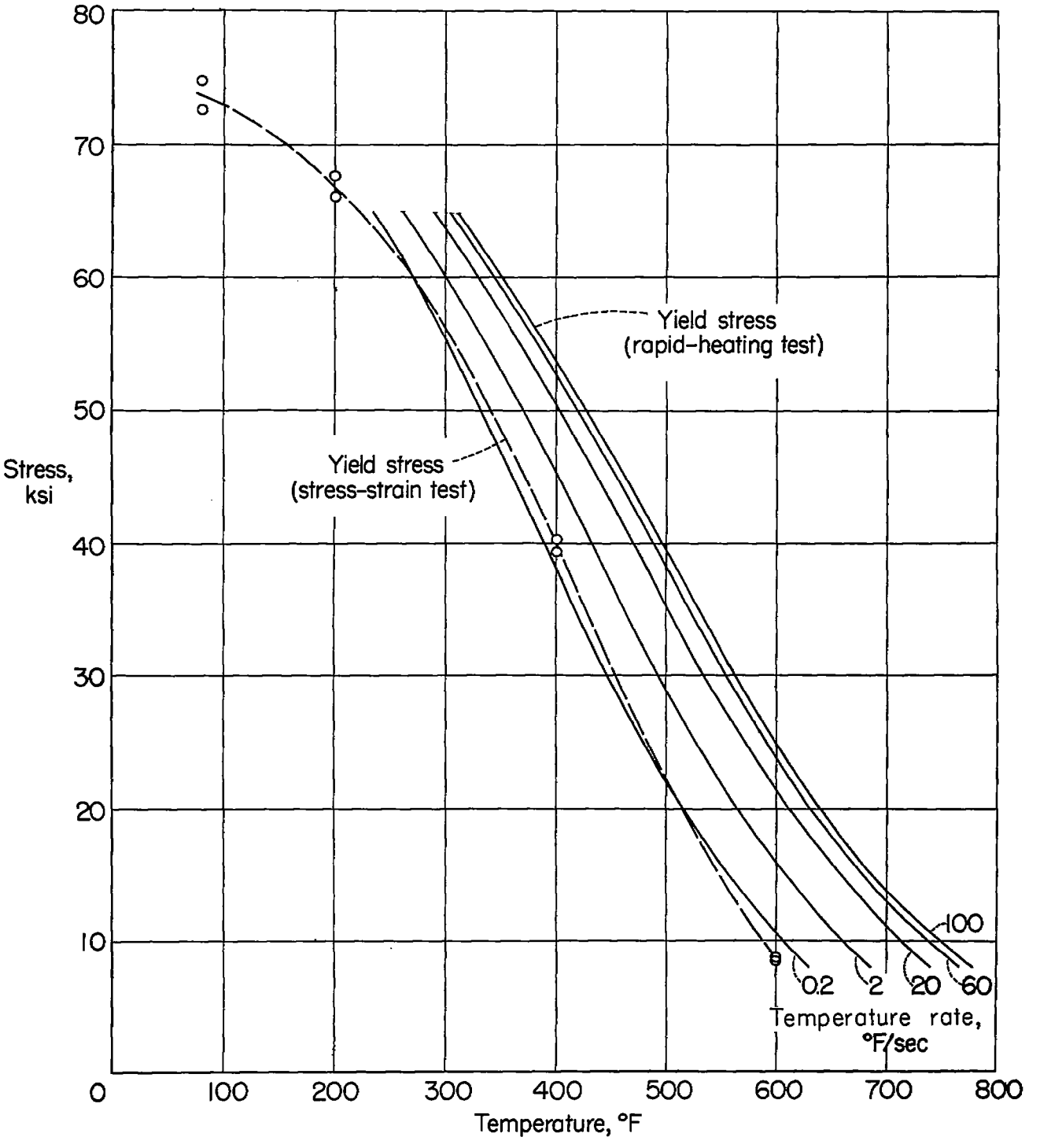

Figure 14.- Tensile yield stress of 7075-T6 aluminum alloy for temperature rates from 0.2° F to 100° F per second and of stress-strain tests for 1/2-hour exposure.

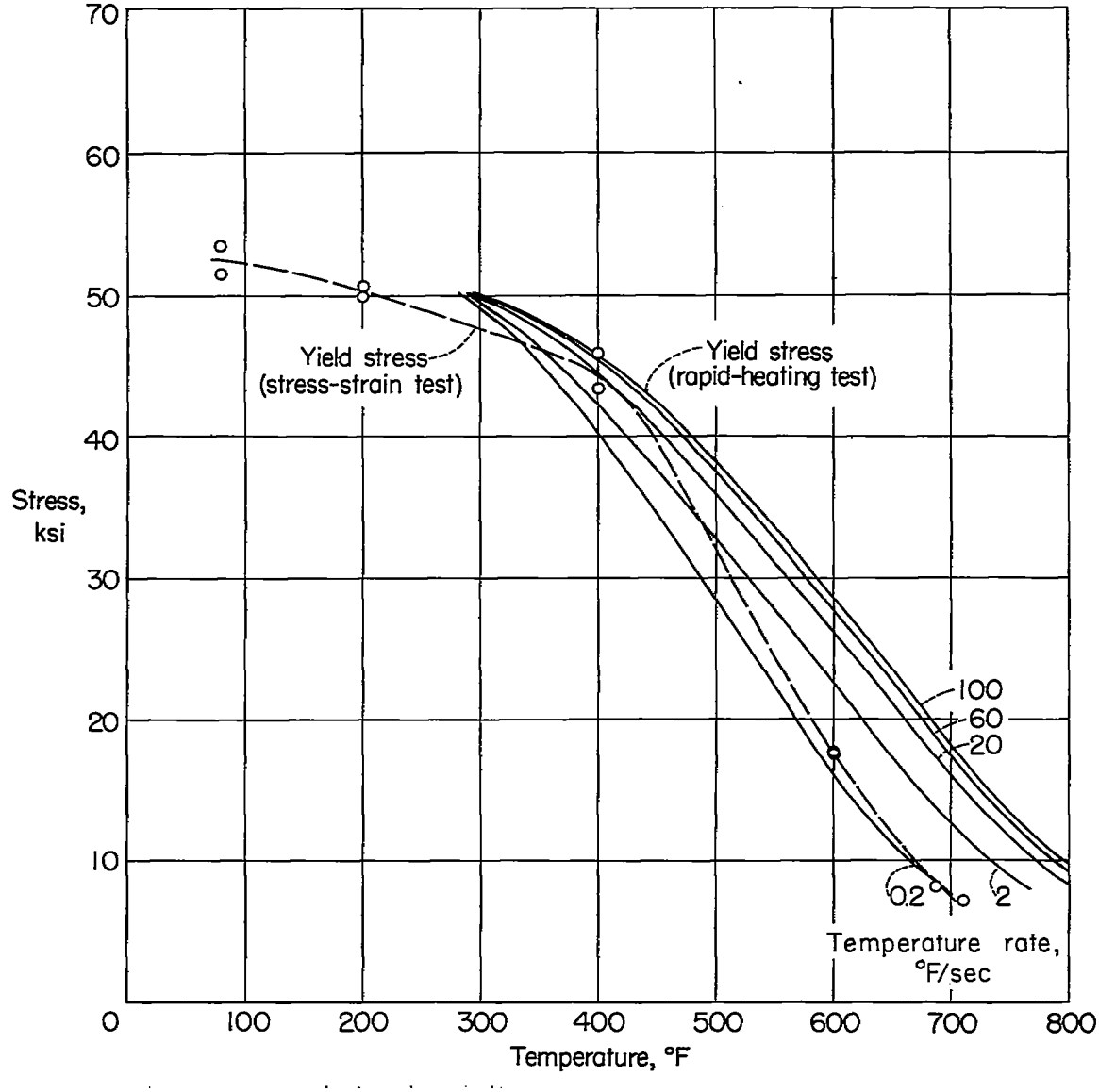

Figure 15.- Tensile yield stress of 2024-T3 aluminum alloy for temperature rates from 0.2° F to 100° F per second and of stress-strain tests for 1/2-hour exposure.

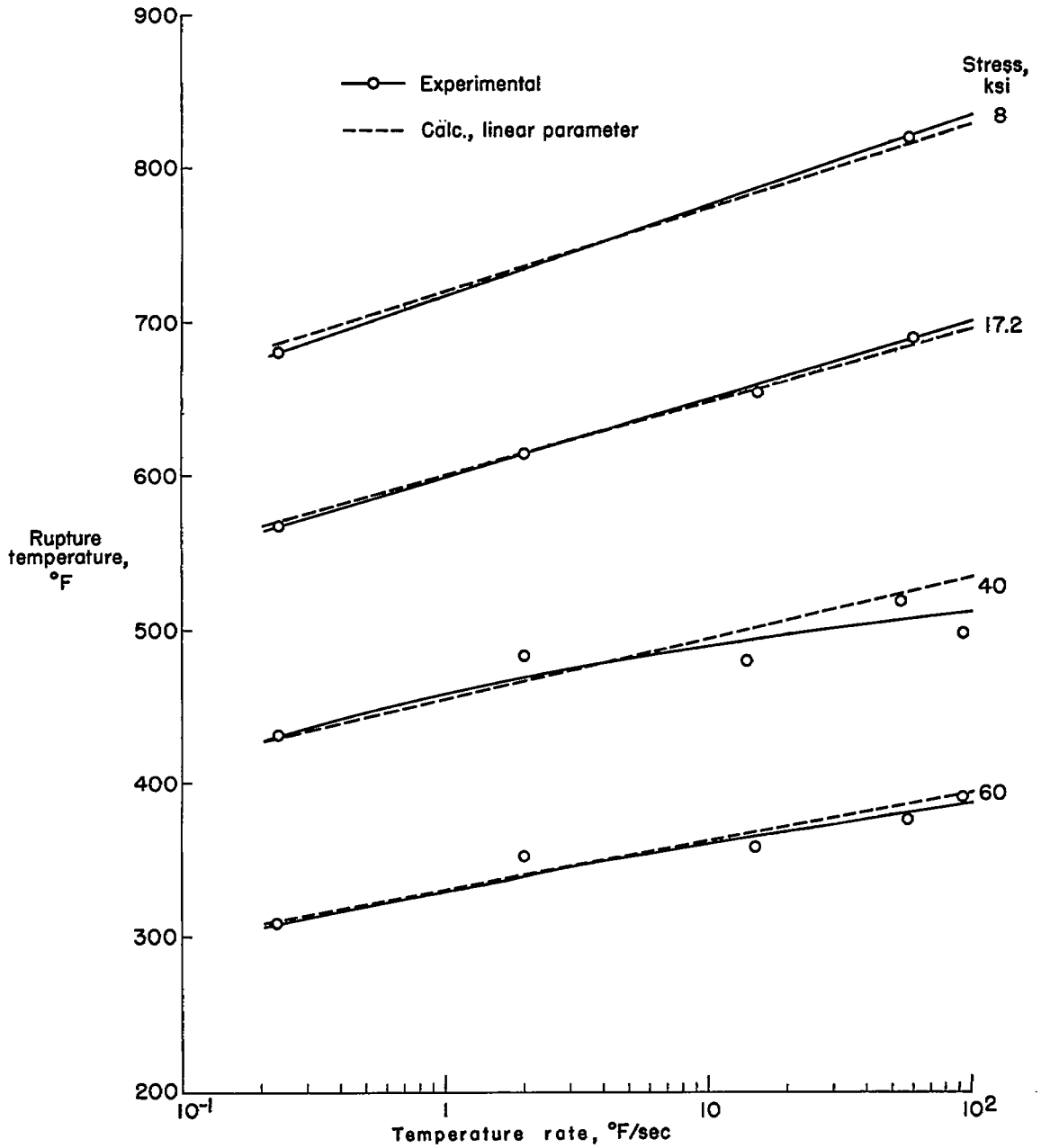

Figure 16.- Experimental and calculated rupture temperatures of 7075-T6 aluminum alloy for temperature rates from 0.2° F to 100° F per second for various stresses.

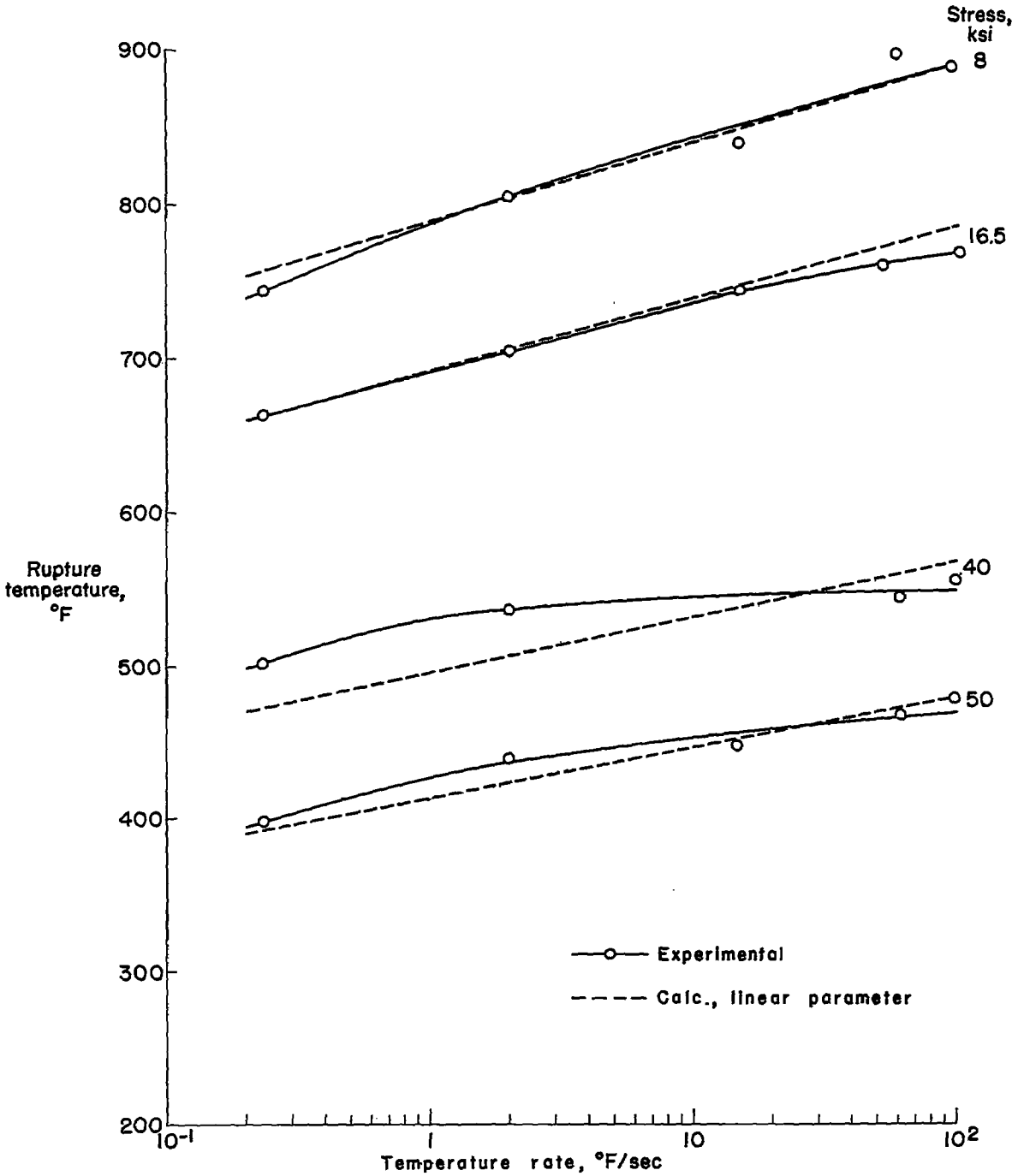

Figure 17.- Experimental and calculated rupture temperatures of 2024-T3 aluminum alloy for temperature rates from 0.2° F to 100° F per second for various stresses.

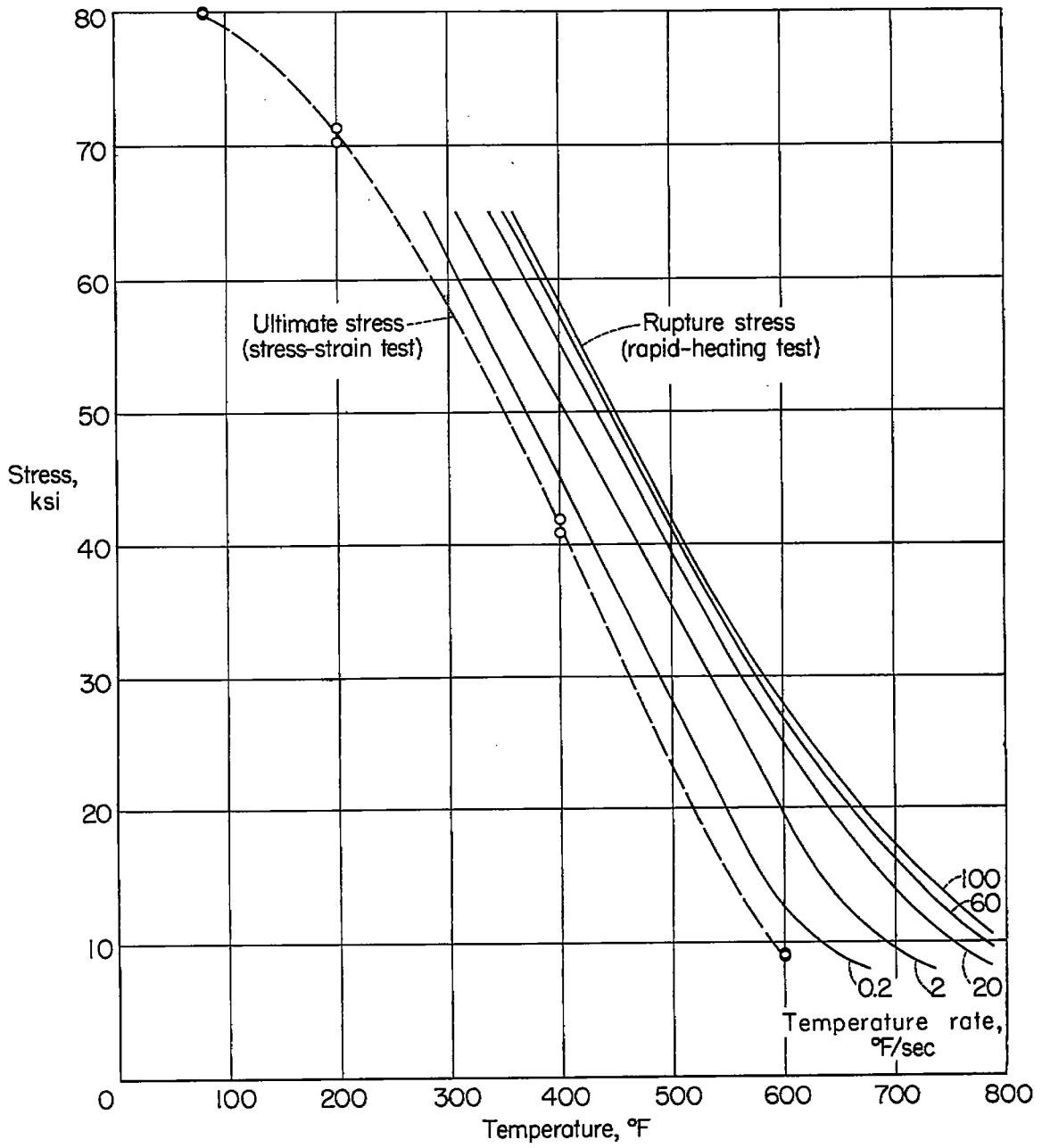

Figure 18.- Tensile rupture stress of 7075-T6 aluminum alloy for temperature rates from 0.2° F to 100° F per second and ultimate tensile stress of stress-strain tests for 1/2-hour exposure.

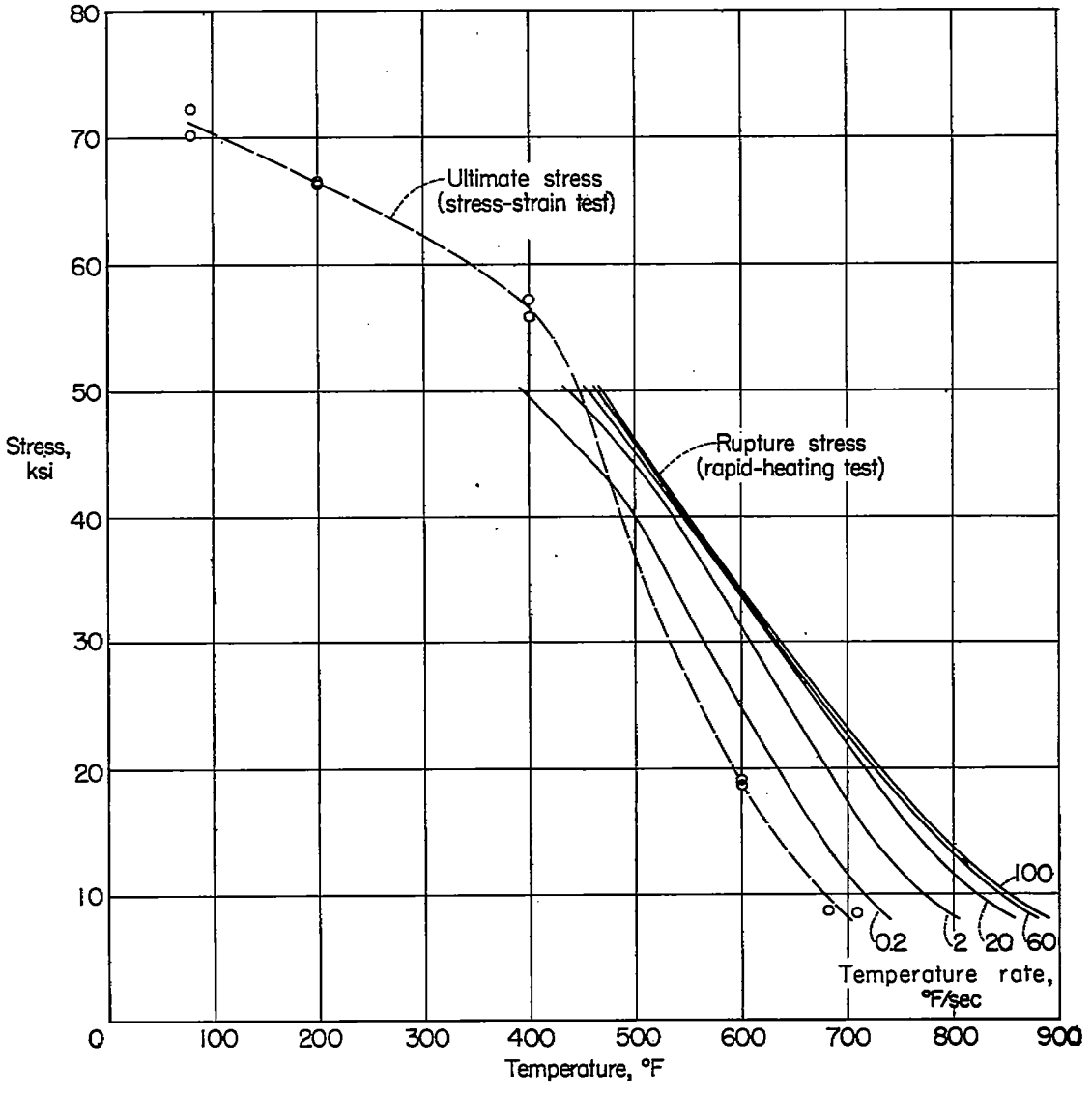

Figure 19.- Tensile rupture stress of 2024-T3 aluminum alloy for temperature rates from 0.2° F to 100° F per second and ultimate tensile stress of stress-strain tests for 1/2-hour exposure.

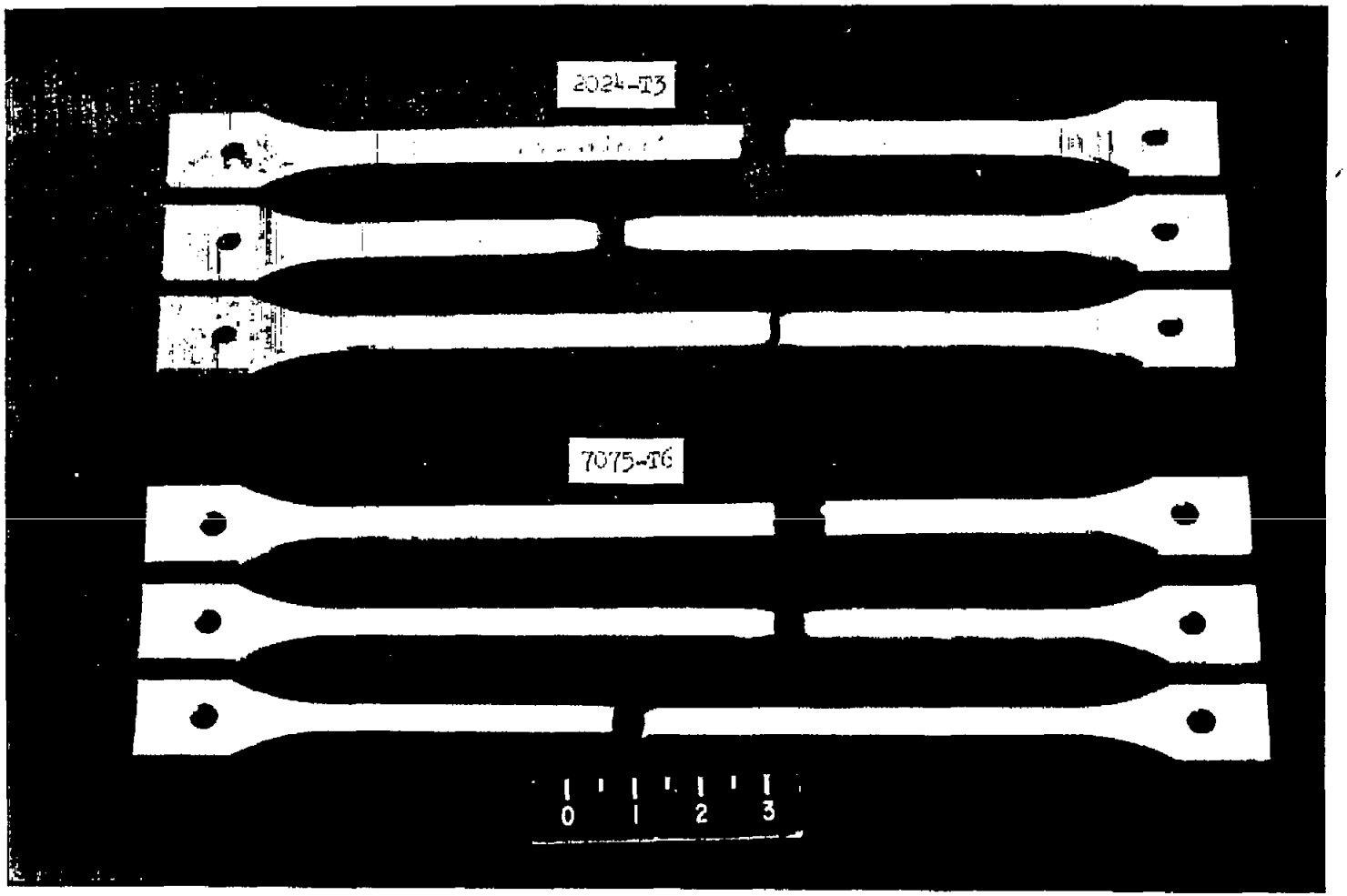

Figure 20.- Fracture of 2024-T3 and 7075-T6 aluminum-alloy specimens. L-85329.1
Stresses increase downward in each group.

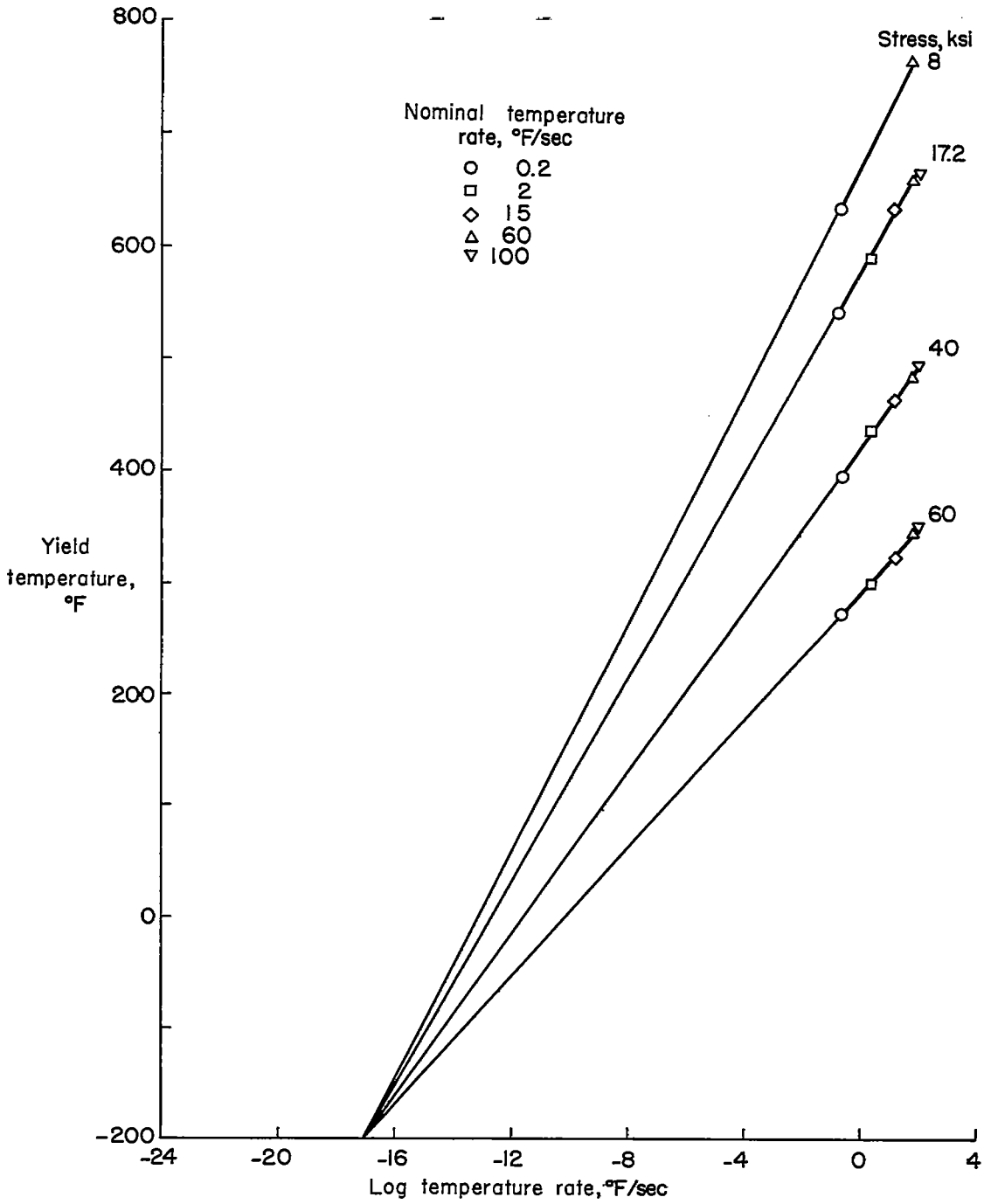

Figure 21.- Variation of yield temperature with logarithm of temperature rate of 7075-T6 aluminum alloy for various stresses.

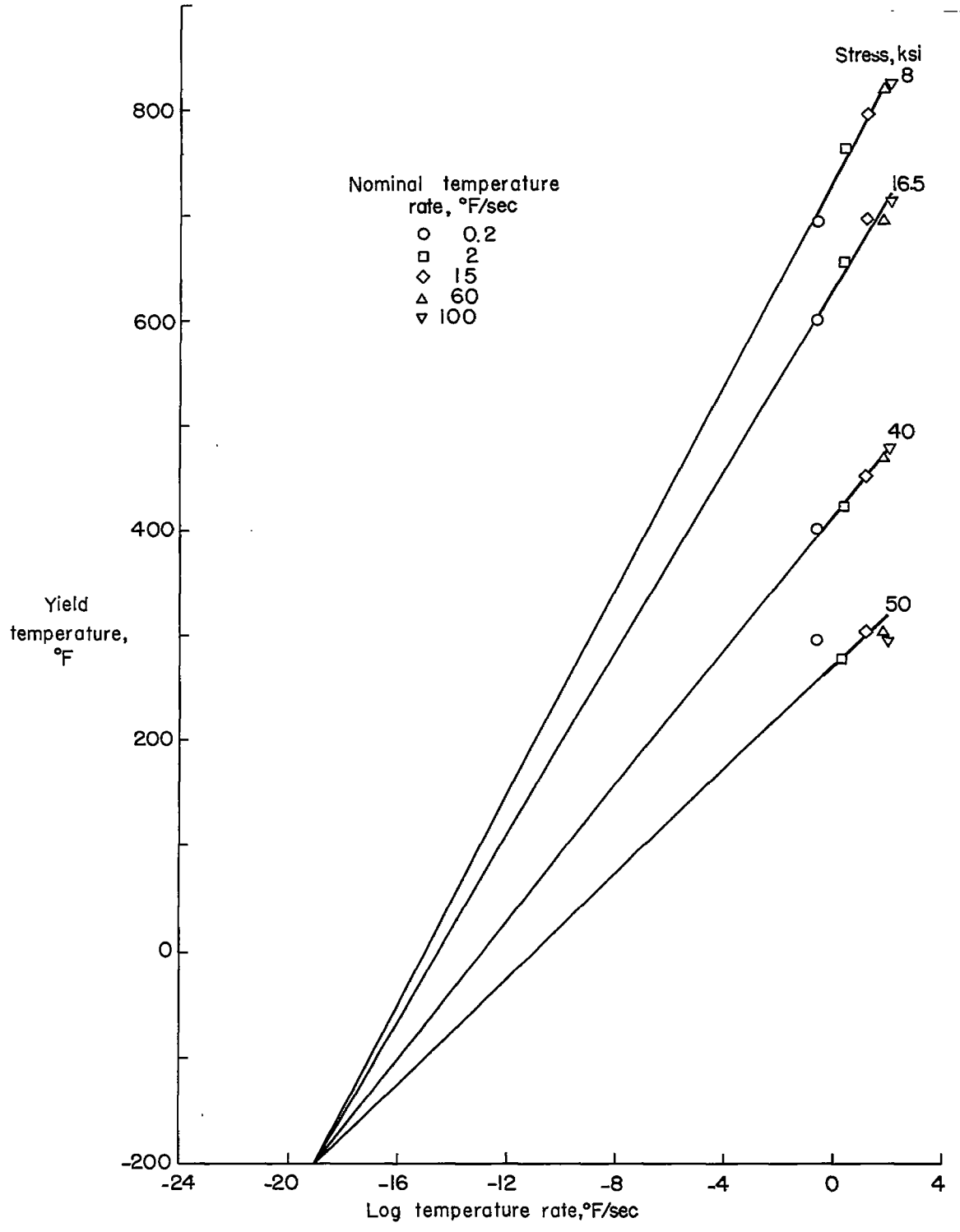

Figure 22.- Variation of yield temperature with logarithm of temperature rate of 2024-T3 aluminum alloy for various stresses.

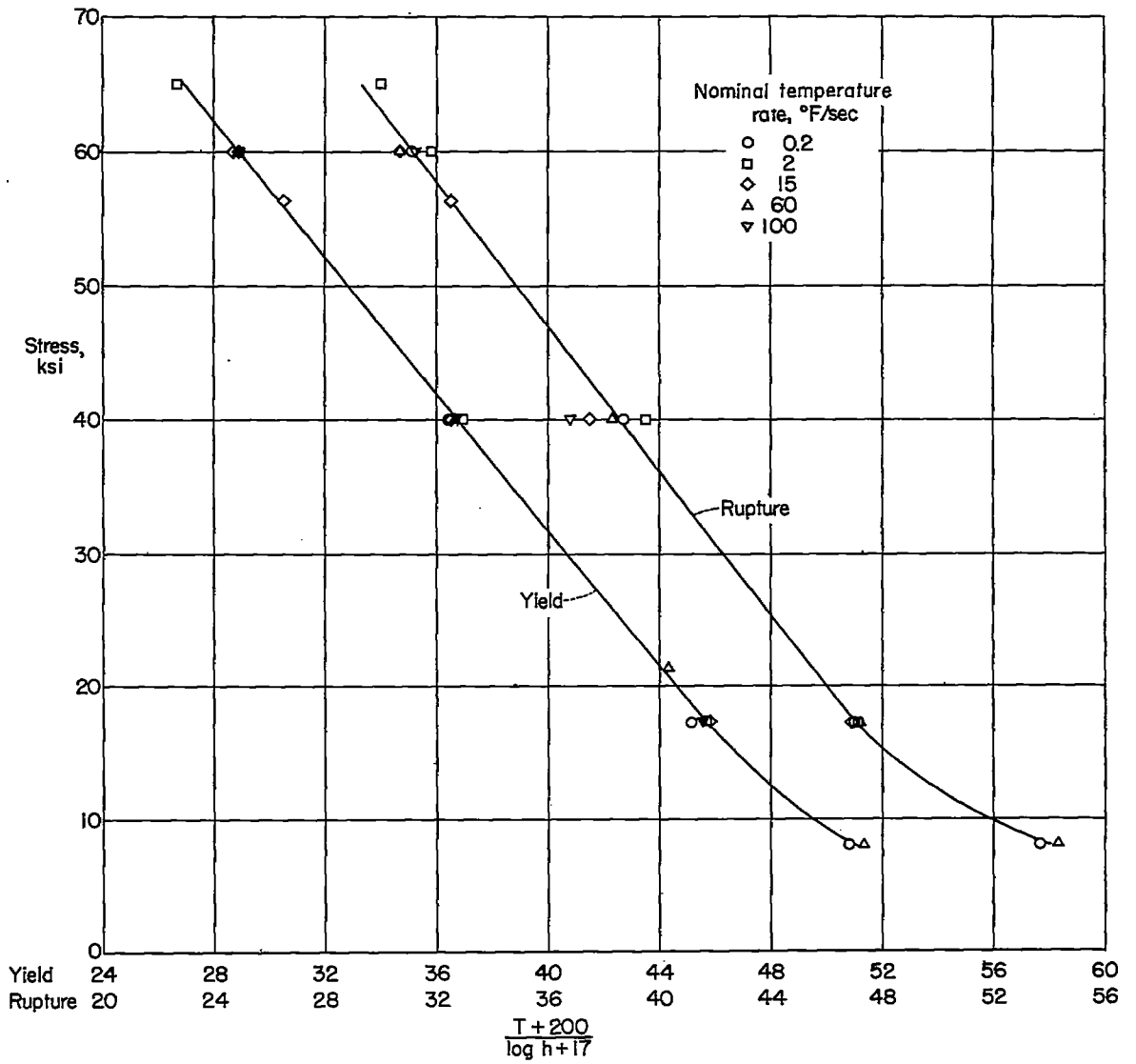

Figure 23.- Master yield- and rupture-stress curves for 7075-T6 aluminum alloy based on linear temperature parameter. (T is in °F and h is in °F per second.)

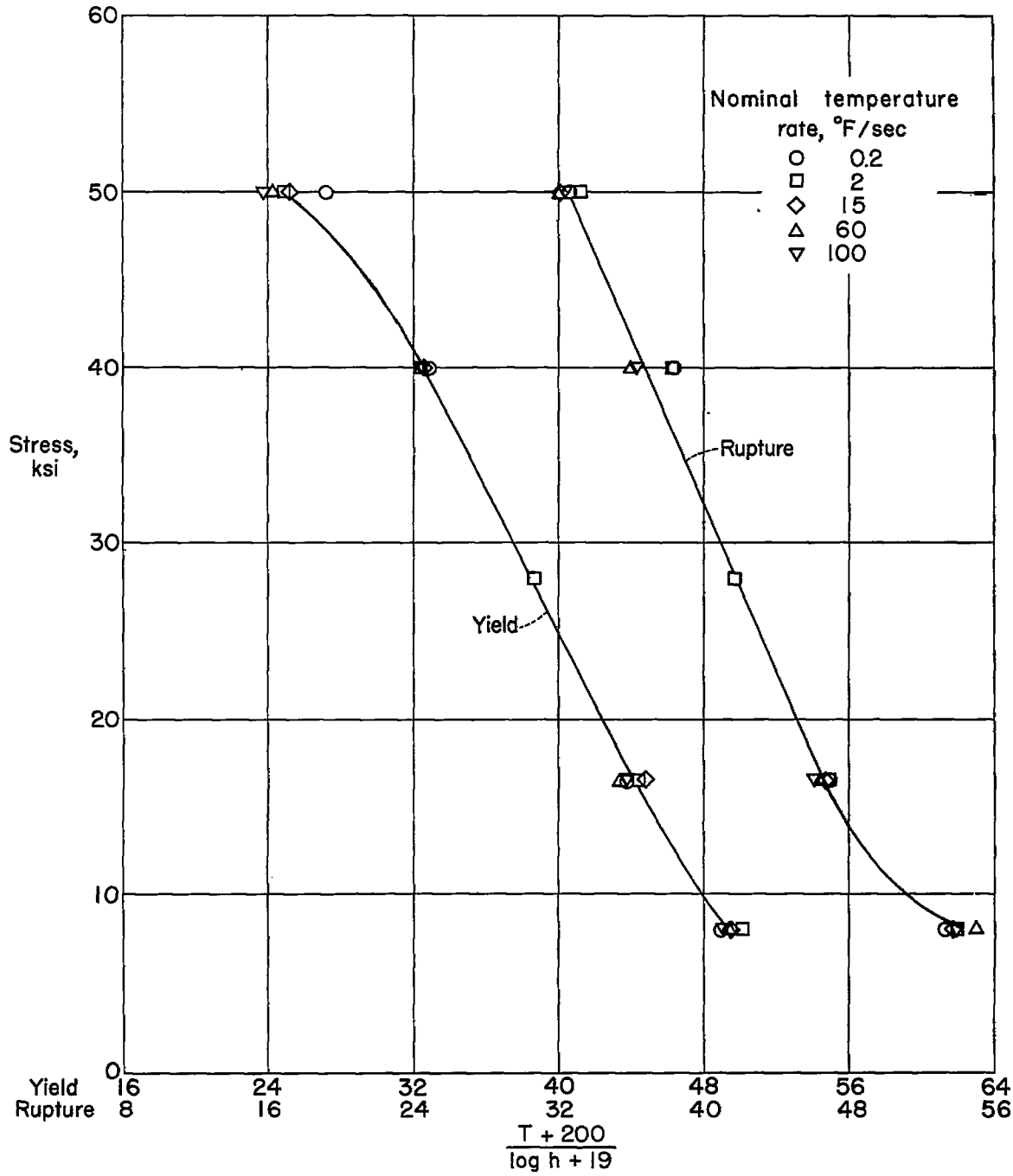

Figure 24.- Master yield- and rupture-stress curves for 2024-T3 aluminum alloy based on linear temperature parameter. (T is in °F and h is in °F per second.)

NACA-Langley - 7-12-55 - 1000